Earthquake Source Imaging: the Past, the Present, the Future

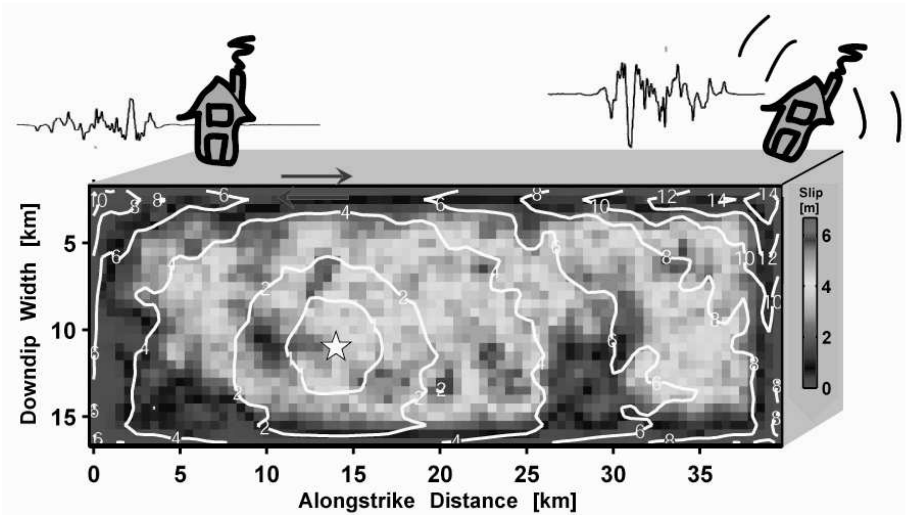

P. Martin Mai & Jean-Paul Ampuero

Institute of Geophysics, ETH Zurich

mai@sed.ethz.chz, ampuero@erdw.ethz.ch

in close collaboration with

S. Jonsson, D. Monelli (all ETH)

G. Festa, B. Delouis and the SPICE Local Scale Task Group

THE LOCAL SCALE EFFORTS

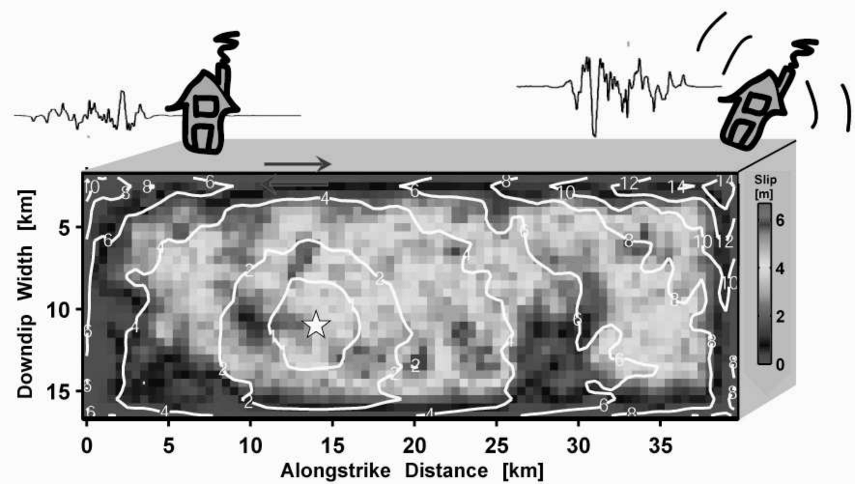

We investigate the processes during an earthquake on (and close to) the fault to better understand the physics of earthquake faulting and the generation of near-source ground motions:

- ► **Source imaging: infer the kinematic properties of earthquake rupture**
- ► **Dynamic rupture modeling: the physics of nucleation, propagation and arrest of earthquake rupture**
- ► **Earthquake scaling: from small to large, from nucleation to arrest**
- ► **Ground-motions and seismic hazard: high-frequency radiation due to earthquake source complexity**

OUTLINE

- ► **A tiny bit of background and theory on earthquake sources and source inversion**

- ► **Database of finite-source rupture models**
  → assessment of variability in rupture models

⇒ **Need for new approaches to rigorously quantify the "quality" of inverted source models, i.e. robustness, resolution, reliability**

- ► **Source Inversion for the 2003 M = 6.6 Bam earthquake**
  → cross-validation between different data sets

- ► **Blind-test for earthquake source inversion**
  → understanding the strength and weaknesses of certain inversion approaches

- ► **Towards dynamically constrained and dynamic source inversion**
  → can we move to dynamic inversions w/o making the additional step of an "intermediate" kinematic inversion?

The "Past": Moment-tensor inversion

► **Although earthquakes occur on rupture planes, one can approximate them as point-sources, represented by a force couple. Recordings of seismic waves can be used to infer the orientation of the forces and their sense of slip.**

Basic types of earthquake faulting

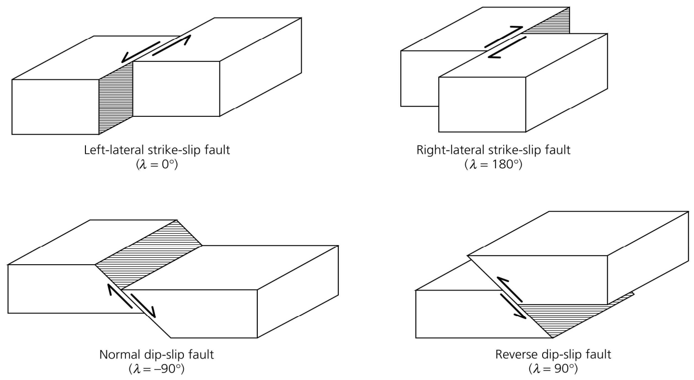

Fault geometry in earthquake studies

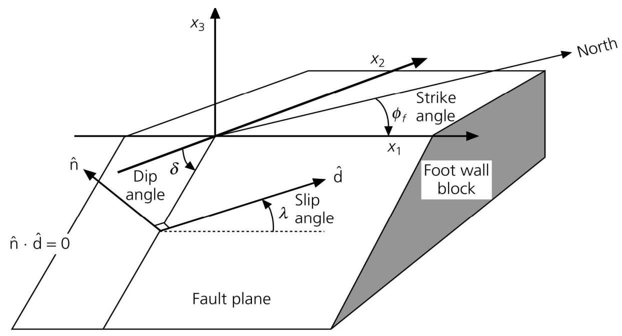

First motions for RL-strike-slip example

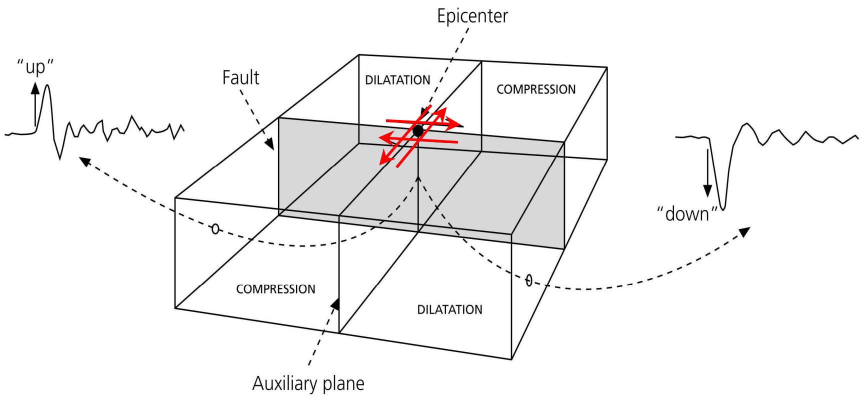

Example moment-tensors

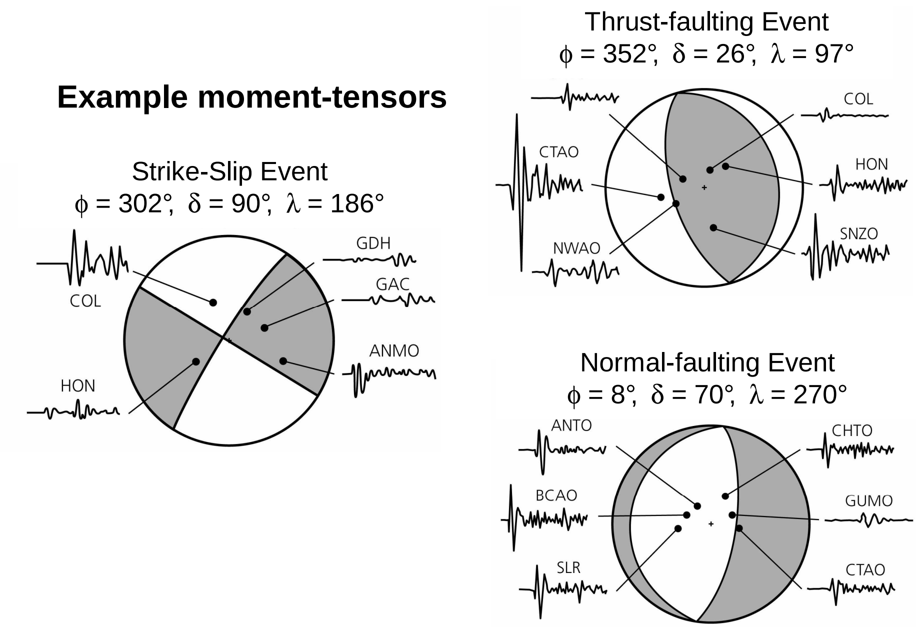

From moment-tensor to finite-faults

► The disadvantage of the moment-tensor representation comes from the point-source approximation and that the time-dependence of the rupture process is largely neglected.

► Validity of point-source representation in the far-field given, but what if we are in the near-field, and have to consider that earthquake ruptures involve fault planes ?

► How to best image and characterize potentially complex rupture histories ?

Rupture Complexity → Double-Couple Point Source

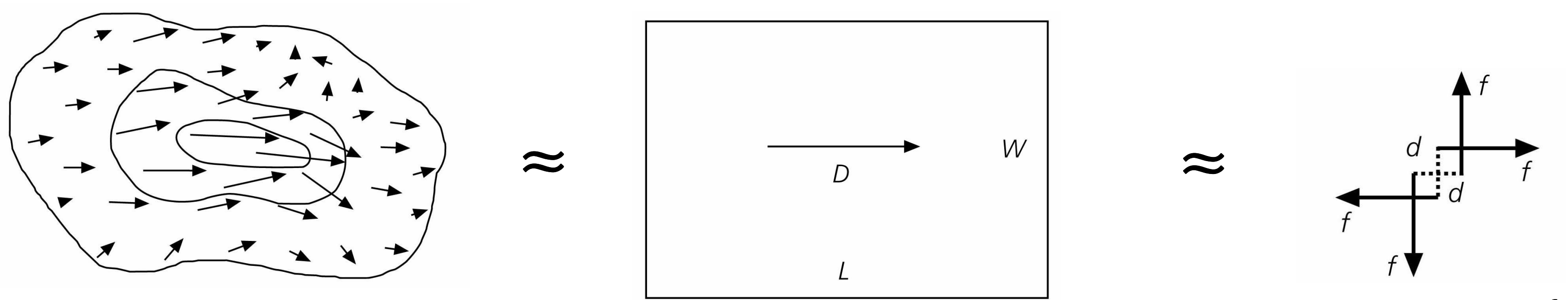

$M = \mu \int D(A)\, dA$

$M = \mu D L W$

$M = f d$

Point-Source → kinematic / dynamic rupture models

"The Present": Finite-Fault Inversion

► The spatio-(temporal) details of the rupture process can be obtained by inverting seismological and/or geodetic (GPS, InSAR) data. The representation theorem links the inelastic displacements in the source region via the Green's functions to the observable ground displacements.

► The representation theorem thus provides a kinematic description of the source without considering the forces and constitutive relations that govern the physics of earthquake rupture (dynamic source modeling)

Representation Theorem: Fractures & Dislocations

- If we consider that earthquakes are produced by fracturing the Earth's crust, generating a dislocation discontinuity Δu at point ξ and time t, we can use the Representation Theorem (in absence of body forces $\mathbf{F}$) to obtain

$$u_i(\mathbf{x}, t) = \int d\tau \int_S \Delta u(\xi, \tau) c_{ijkl} \nu_j G_{nk,l}(\xi, \tau; \mathbf{x}, t)\, dS. \quad (10)$$

- Equation [10] serves to define a kinematic source model, in which the deformations $\mathbf{u}$ are derived from given/known/assumed slip vector Δu that represents the inelastic displacement of the two sides of a fault of surface S.

observed displacement (what we have)

displacement history on fault (what we want)

elasticity tensor (what we need)

Green's tensor for geometry of interest (what we need)

"The Present": Finite-Fault Inversion

► "Standard" approach to earthquake source imaging

$$u_n(\mathrm{x},t) = \sum_{itm=1}^{ntm} \sum_{is=1}^{ns} \sum_{if=1}^{nf} m(if,is,itm) \times \int \left[u_{\mathrm{unit}_{tr}}(\tau - \Delta t_{\mathrm{trig}}) \right] \times c_{i(is)jkl}(\xi) n_j G_{kn,l}(\mathrm{x}, t-\tau; \xi(if), 0)\, d\tau,$$

$$\Delta t_{\mathrm{trig}} = \frac{R}{Vr} + \Delta tw \cdot (itm - 1).$$

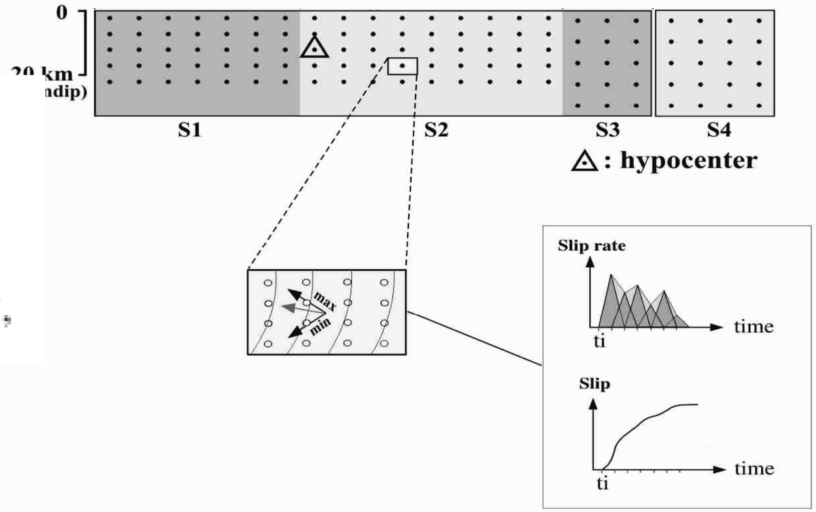

-- planar fault surface (or several planar segments), subdivided into many small elements

-- characterize displacement history in each subfault by slip occurring in several time windows

-- express the spatio-temporal faulting process as a summation of elementary slip functions, weighted for each subfault and each time window

-- array *m(if,is,itm)* is slip on the *i*th subfault, in the *is*th direction for the *itm*th time window

-- R is the distance of each subfault from the hypocenter, Δt_{trig} the onset time when each subfault starts slipping, computed for fixed rupture velocity

-- There are *nf* subfaults, *ns* slip directions, *ntm* time windows.

→ Assuming constant rupture velocity v_r and rise time τ_r, the problem is linear. If this assumption is relaxed, inversion becomes non-linear!

→ Usually, simple slip-velocity functions are used (off-set by using many time windows)

"The Present": Finite-Fault Inversion

- The linearized scheme can obviously written in "standard" notation

$$\underline{d} = \underline{\underline{G}}\,\underline{m}$$

$$\begin{bmatrix} d_1 \\ d_2 \\ \vdots \\ \\ d_1 \\ d_2 \\ \vdots \\ \\ d_1 \\ d_2 \\ \vdots \end{bmatrix} \cong \begin{bmatrix} G_{11} & G_{12} & \cdots & G_{1m} \\ G_{21} & G_{22} & \cdots & G_{2m} \\ \vdots & \vdots & & \\ & & & \\ G_{11} & G_{12} & \cdots & G_{1m} \\ G_{21} & G_{22} & \cdots & G_{2m} \\ \vdots & \vdots & & \\ & & & \\ G_{11} & G_{12} & \cdots & G_{1m} \\ G_{21} & G_{22} & \cdots & G_{2m} \\ \vdots & \vdots & & \end{bmatrix} \begin{bmatrix} s_1 \\ s_2 \\ \vdots \\ \vdots \\ s_m \end{bmatrix}$$

(time) data points station 1

(time) data points station N

Subfault 1 synthetics

Subfault 2 synthetics

Subfault m synthetics

Dislocation in subfault 1

Dislocation in subfault 2

Dislocation in subfault m

"The Present": Finite-Fault Inversion

► For linear problems, it is straightforward to apply regularization by adding smoothing or damping constraints (now also including an error term ε)

$$\begin{pmatrix} \underline{d} + \underline{\varepsilon} \\ \underline{\varepsilon}_c \end{pmatrix} = \begin{pmatrix} \underline{\underline{G}} \\ \lambda \underline{\underline{S}} \end{pmatrix} \underline{m}$$

- **S** could be a temporal or spatial smoothing constraints, a roughness minimization in form of a finite-difference operator, or in principal any other *a priori* information useful to constrain the linear model
- The value of the hyper-parameter λ needs to be found; "classical" techniques use trade-off curves, alternative, more statistically sound approaches, use for instance the Akaike Bayesian Information Criterion (ABIC, *Akaike, 1980; Yabuki and Matsu'ura, 1992*)

$$\mathrm{ABIC} = -2\log\left[\int P(\mathbf{d}\,|\,\mathbf{m},\sigma)P(\mathbf{m},\sigma')\mathrm{d}\mathbf{m}\right] + 2N_{\mathrm{hp}}$$

$$P(\mathbf{d}\,|\,\mathbf{m},\sigma) = (2\pi\sigma^2)^{-\frac{M}{2}}\exp\left[-\frac{\|\mathbf{d}-\mathbf{A}\mathbf{m}\|^2}{2\sigma^2}\right],$$

$$P(\mathbf{m},\sigma') = (2\pi\sigma'^2)^{-\frac{M_s}{2}}\exp\left[-\frac{\|\mathbf{S}\mathbf{m}\|^2}{2\sigma'^2}\right],$$

P(): likelihood functions for data and *a priori* information on the model parameters
N: total number of model parameters
N_{hp}: number of hyper-parameters
M: number of data
M_s: number of smoothing constraints

"The Present": Finite-Fault Inversion

► Let us relax the assumption of fixed, constant rupture velocity and fixed, constant rise time. We seek to find the exact time when each point of the fault starts to slip, and for how long, and perhaps also with a complex trajectory (i.e. a complex, spatially variable slip-velocity function).

Slip on the fault plane

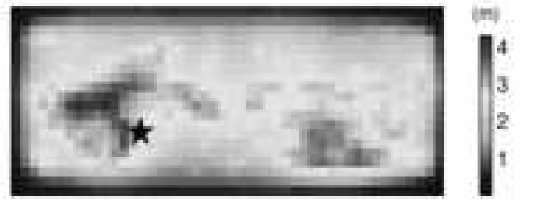

Rupture onset times

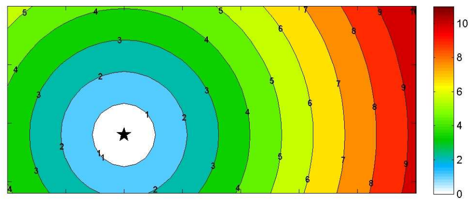

Rise time

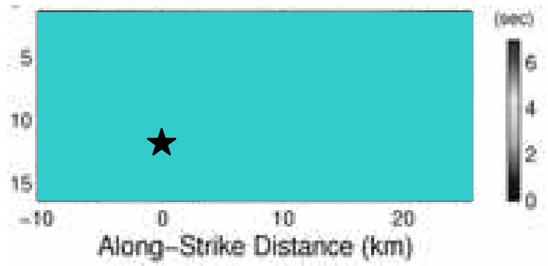

SVF's from dynamic modeling

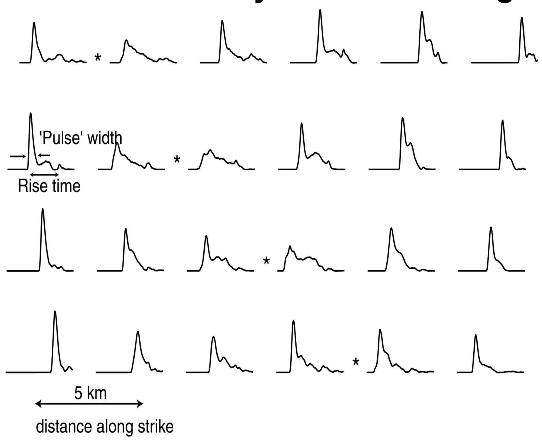

Alternative SVF's

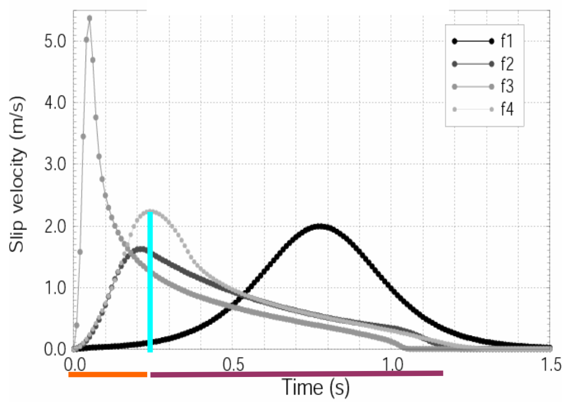

$$T_p + T_d = \tau_r$$

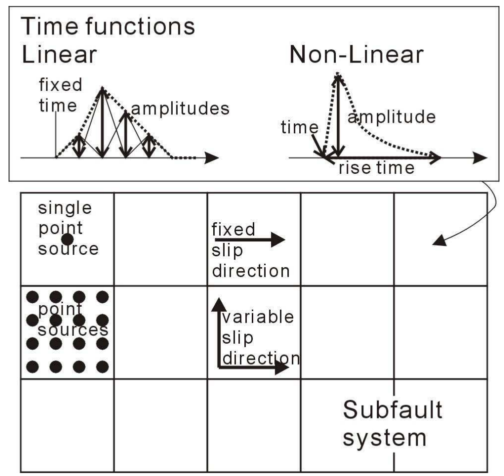

Source Model Database

► Online database of kinematic rupture models

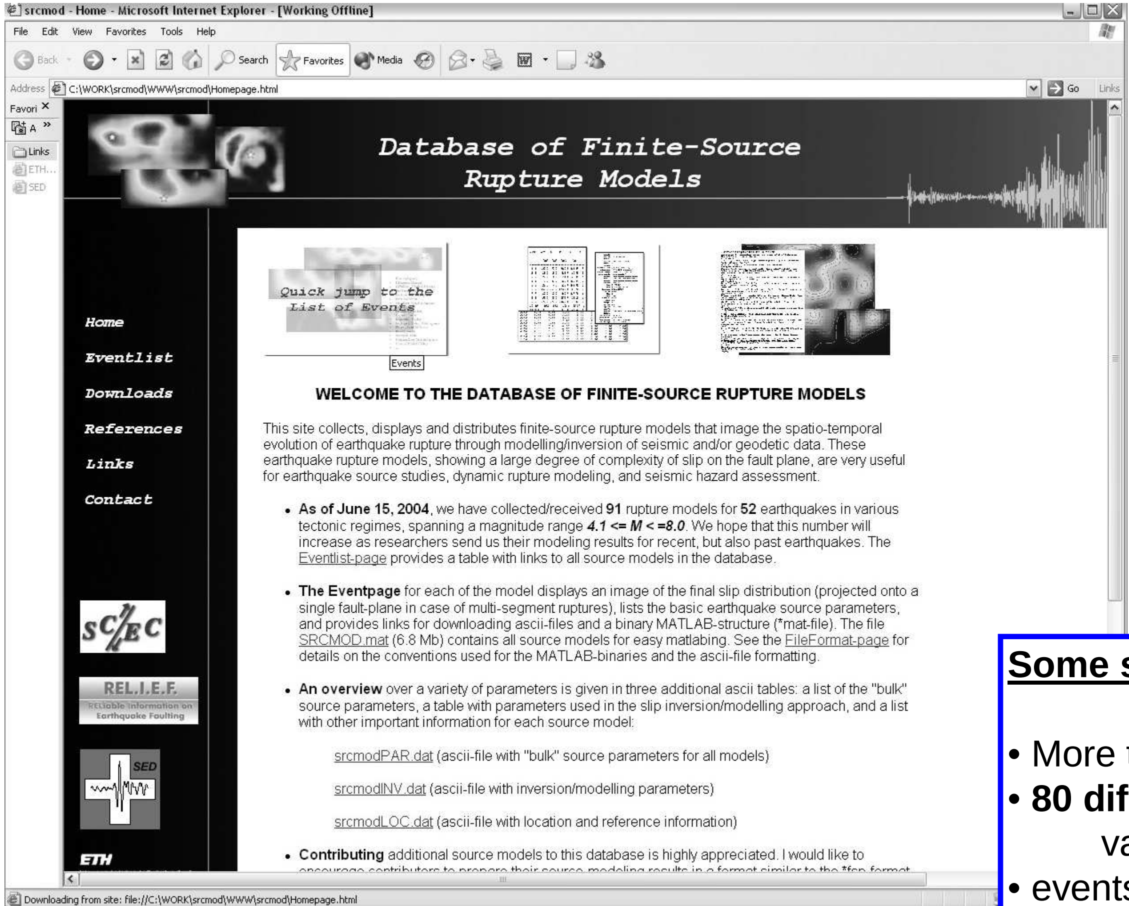

http://www.seismo.ethz.ch/srcmod

Potency-area scaling for all source-models

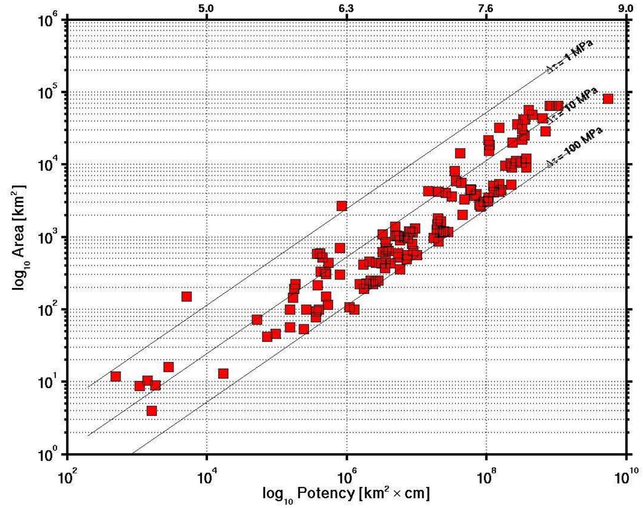

<u>Some statistics</u>: So far, we have collected

- More than **140 rupture models** for
- **80 different** earthquakes that occurred in various tectonic regimes
- events span the magnitude range **4.1 ≤ M ≤ 8.9**
- **30** events have **more than one** published source model
- more than **20** researchers contributed to this database by sending their source models.

Source Model Database

- **Online database of kinematic rupture models**

http://www.seismo.ethz.ch/srcmod

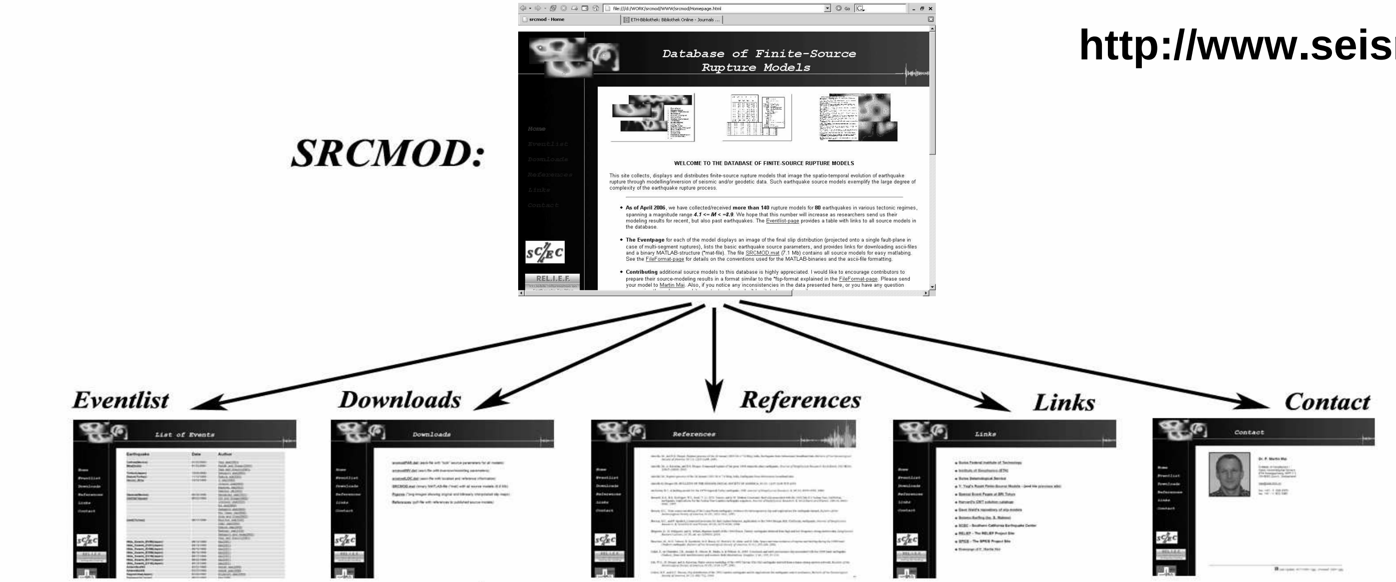

For each rupture model, there is …

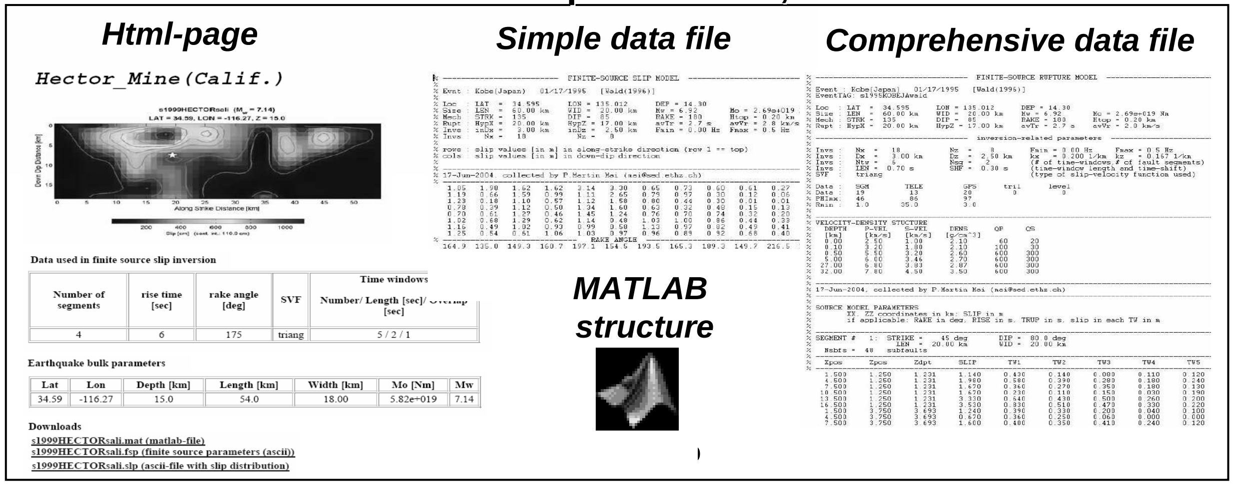

Eidgenössische Technische Hochschule Zürich

Source Model Database

► Useful to study earthquake scaling and source-rupture properties in general

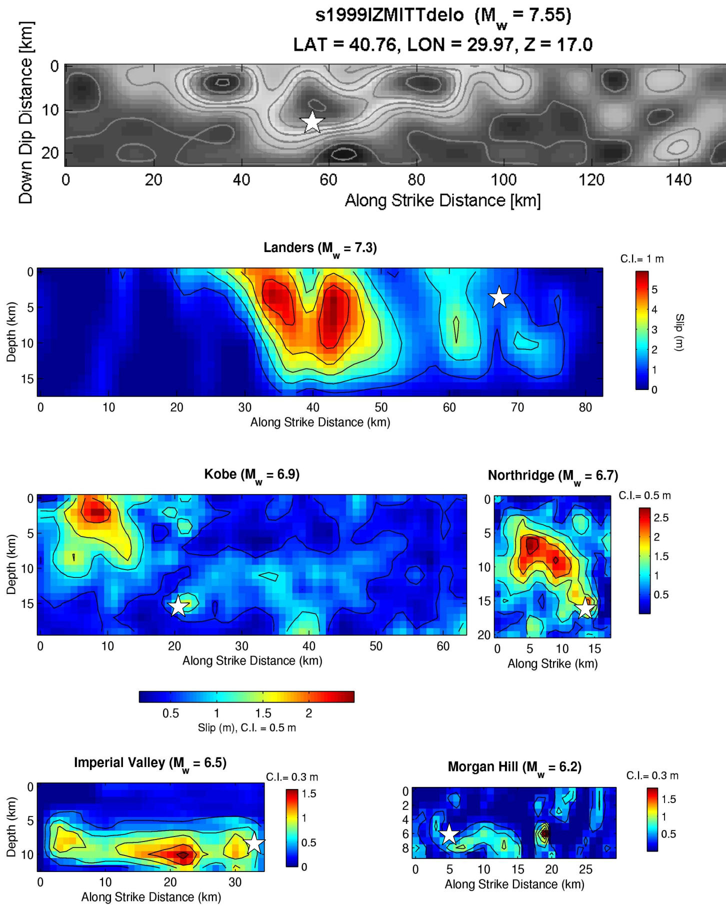

Earthquake slip is heterogeneous at all spatial scales

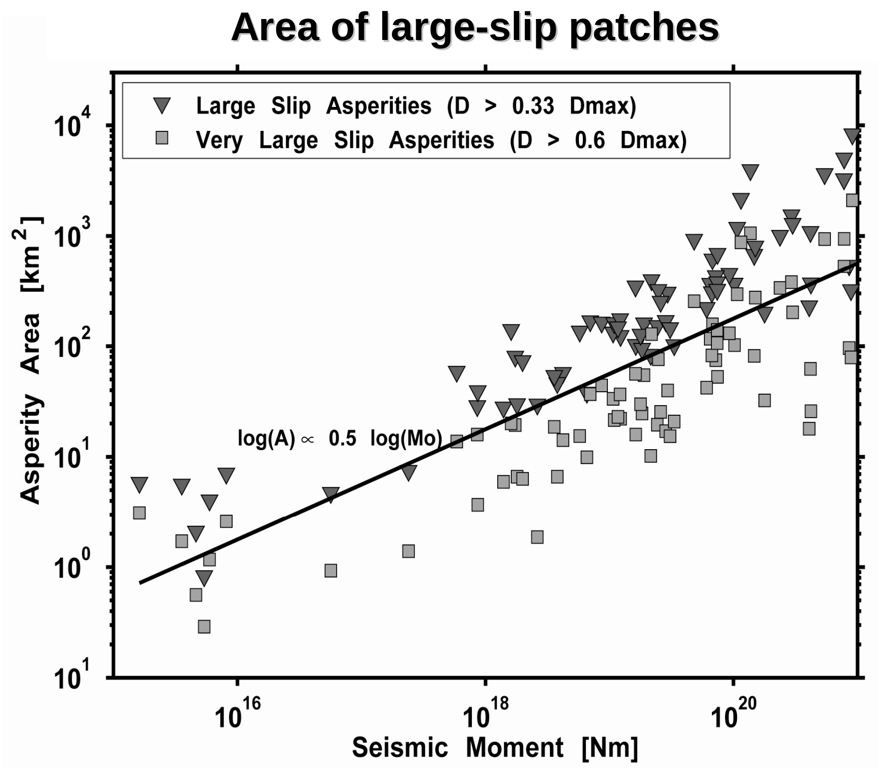

Source Model Database

► Appreciate the <u>difference</u> in rupture models for a single event: the case of the 1999 Izmit earthquake

Delouis et al (2002), M = 7.58

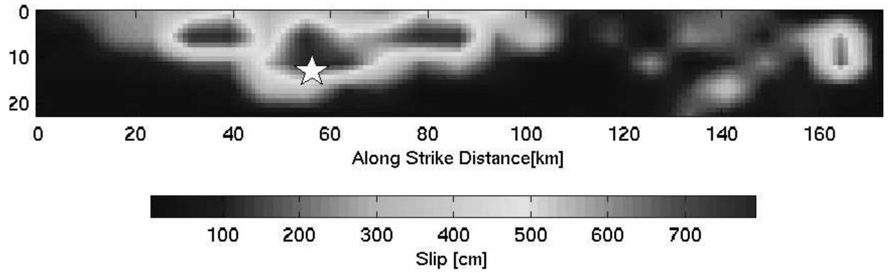

Yagi and Kikuchi (1999), M = 7.42

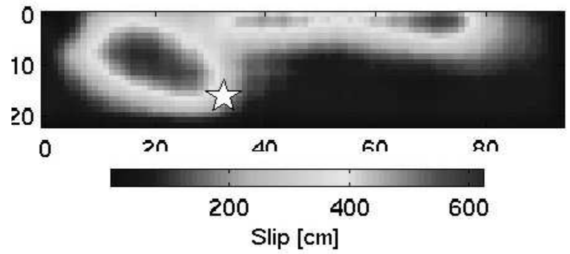

Sekiguchi and Iwata (2002), M = 7.41

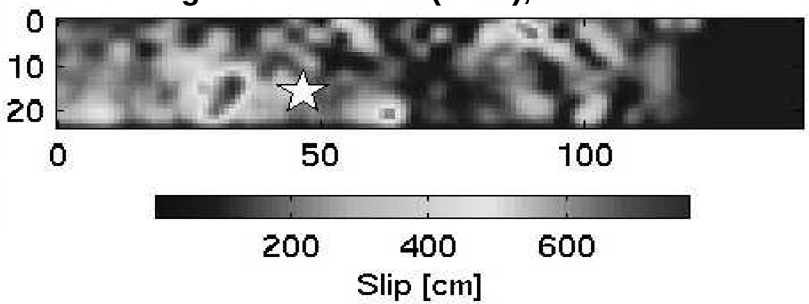

Bouchon et al (2002), M = 7.61

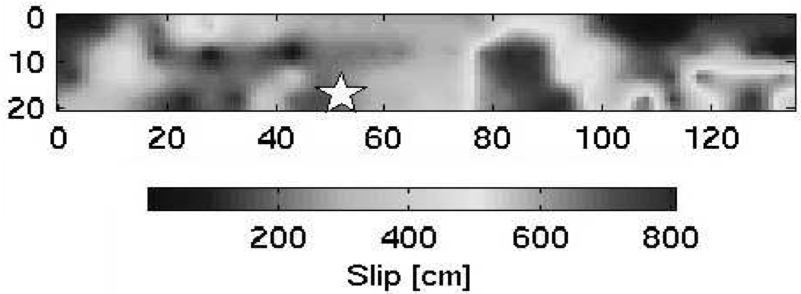

→ What drives the large differences between these slip models? The number of near-source recordings is very limited, 10 stations at distance up to ~80 km !

Source Model Database

► Appreciate the <u>similarities</u> in rupture models for a single event: the case of the 1999 Chi-Chi earthquake

Chi et al. (M = 7.71)

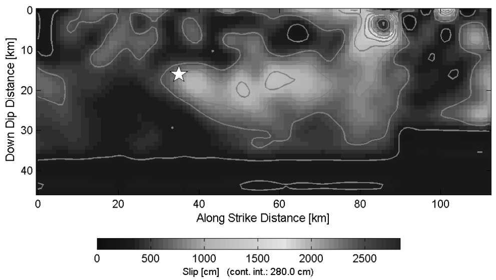

Sekiguchi et al. (M = 7.62)

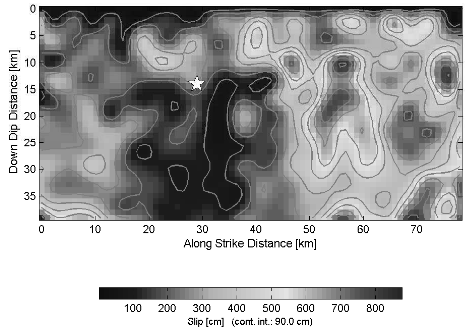

Ma et al. (M = 7.72)

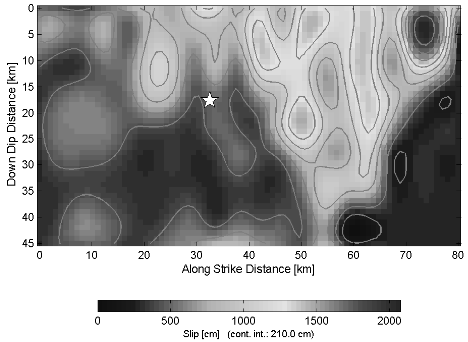

Wu et al. (M = 7.72)

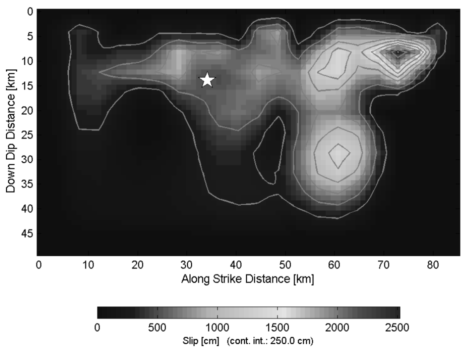

Zeng et al. (M = 7.66)

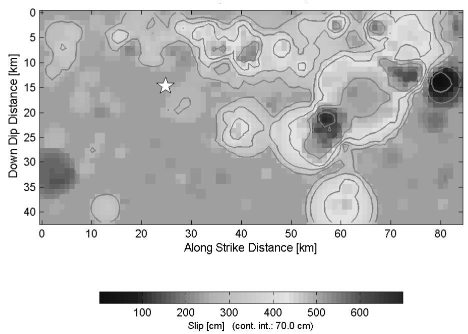

Johnson et al. (M = 7.66)
(GPS data only)

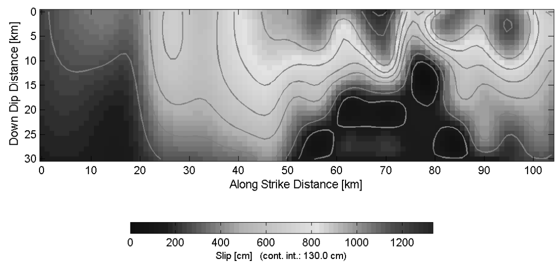

→ **As the data coverage increases (441 strong-motion stations, 60 within 20 km of the fault trace), the models start to become more similar, at least in their general features**

Source process of the 2003 Bam earthquake from inversion of seismic recordings and InSAR data

P. Martin Mai[1], Sigurjón Jónsson[1], David Small[2] and Jerome Salichon[1]

[1] *Institute of Geophysics, ETH Zürich, Switzerland*

[2] *Remote Sensing Laboratories, Univ. of Zürich*

The Dec 26, 2003, Bam earthquake

- Magnitude 6.6
- The first large earthquake in Bam for > 2500 years
- Almost 70% of all buildings destroyed
- Death toll > 26’000
- Vertical ground acceleration exceeded 1g in Bam
- RL-strike-slip on a NS-oriented, nearly vertical fault,
- No major surface rupture, only minor cracks
- Not on the known Bam fault

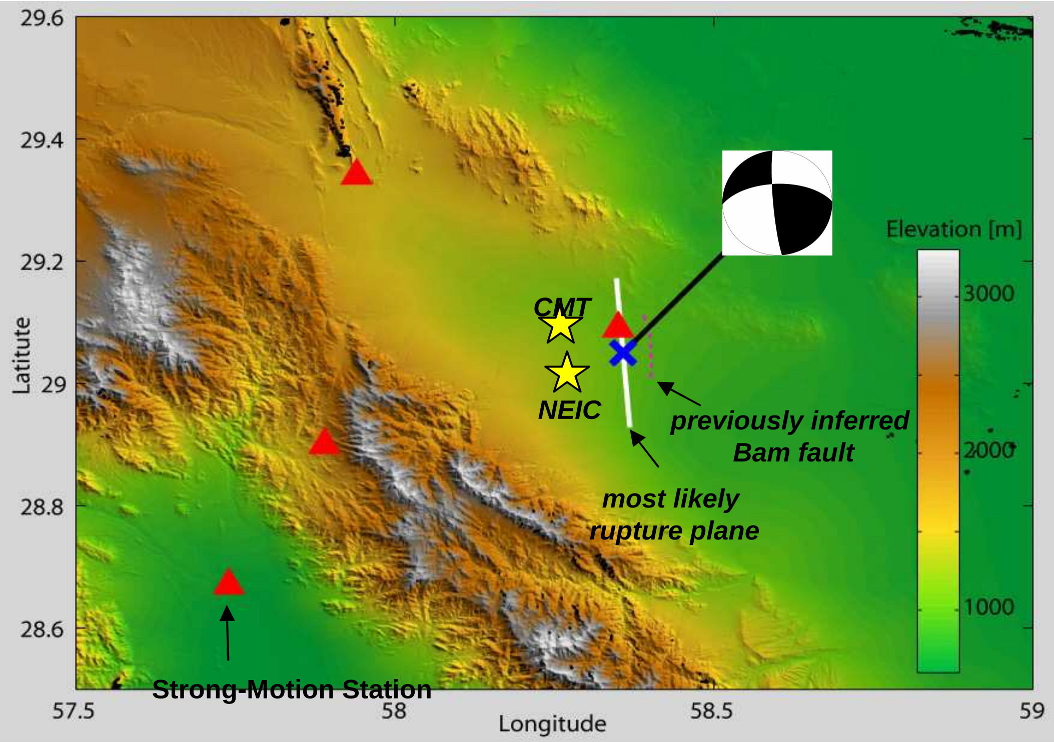

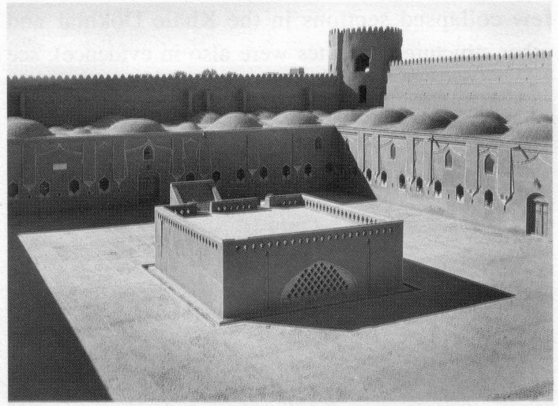

Arg-e Bam; From Langenbach, 2004

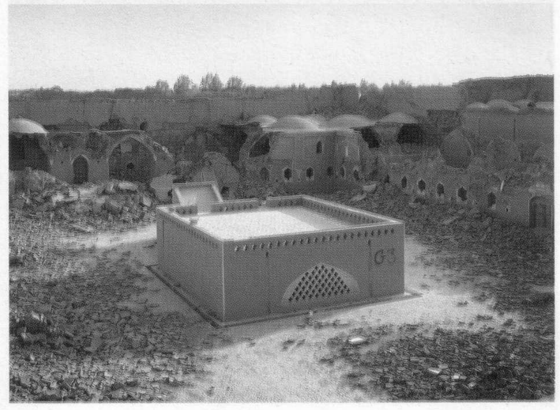

Bam Source Inversion

- ► Envisat satellite interferometric radar (InSAR) data to constrain fault location, fault geometry and distributed slip on the fault plane

- ► Teleseismic data (P- and SH-waves) to derive an independent model of the slip distribution and to constrain the temporal rupture evolution

- ► **“Cross-validation”:** how well does the teleseismic solution predict the permanent displacement field? Can the InSAR solution be used as a constraint in the teleseismic inversion?

- ► We further try to model the near-source strong motion record in the city of Bam, based on the InSAR and teleseismic inversion results

Envisat InSAR data

Descending orbit
(03/12/2003 – 11/02/2004)

Ascending orbit
(16/11/2003 – 29/02/2004)

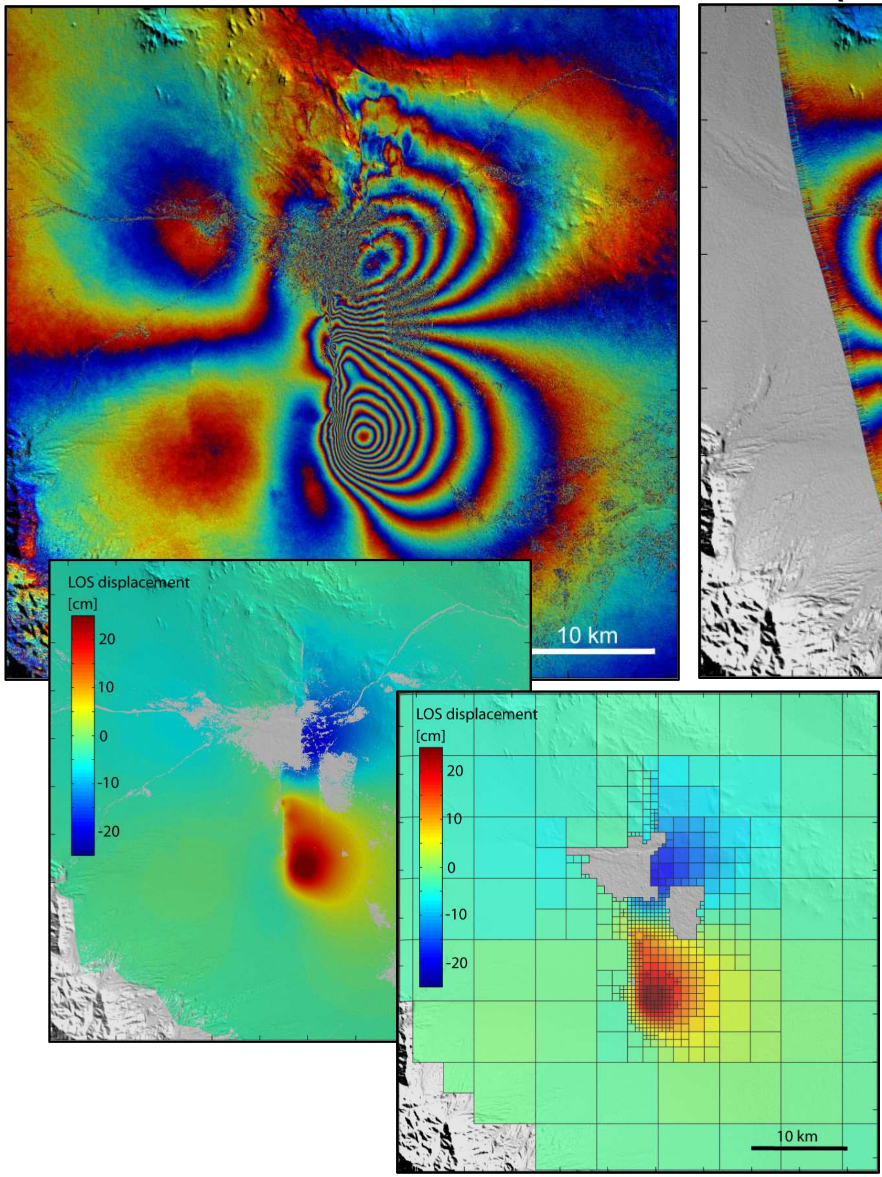

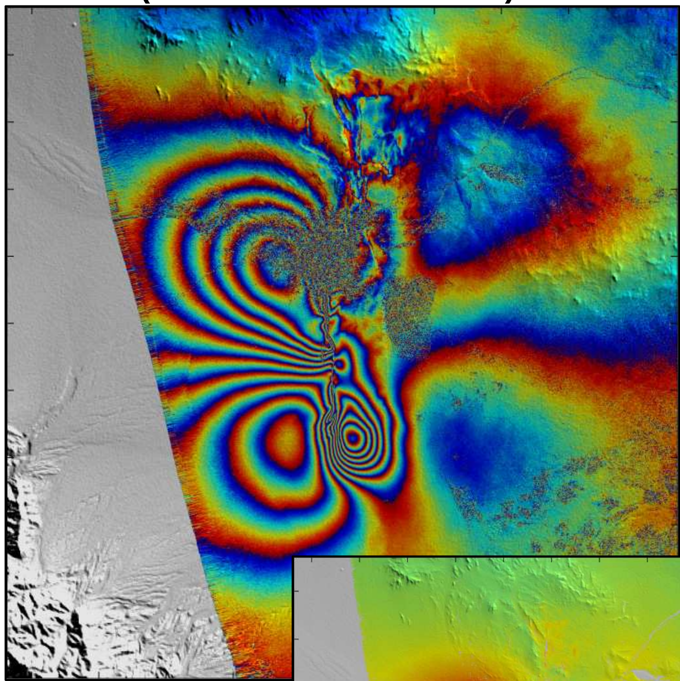

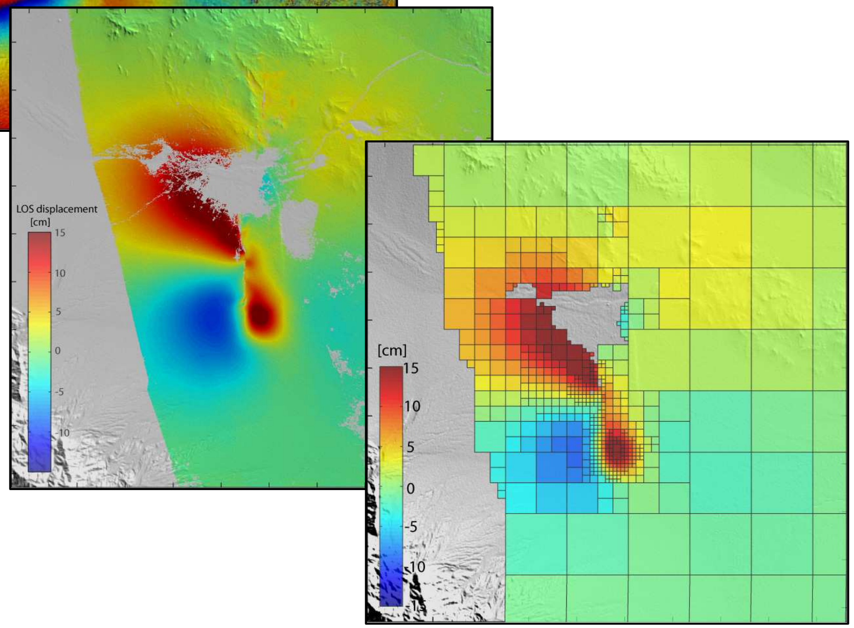

- Topography removed
- Bam and Baravat decorrelated
- Maximum LOS displacement ~30 cm (desc), ~ 15 cm (asc.)
- Discontinuities south of Bam
- Interferograms unwrapped
- Quadtree subsampling to reduce to 600 - 700 points

Geometry by Nonlinear Optimization

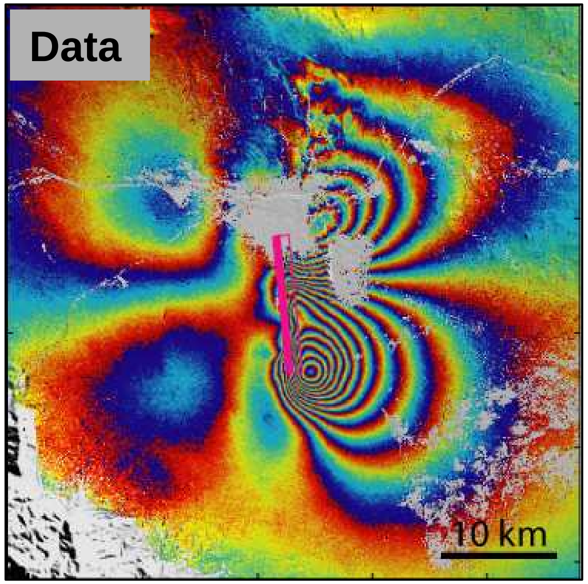

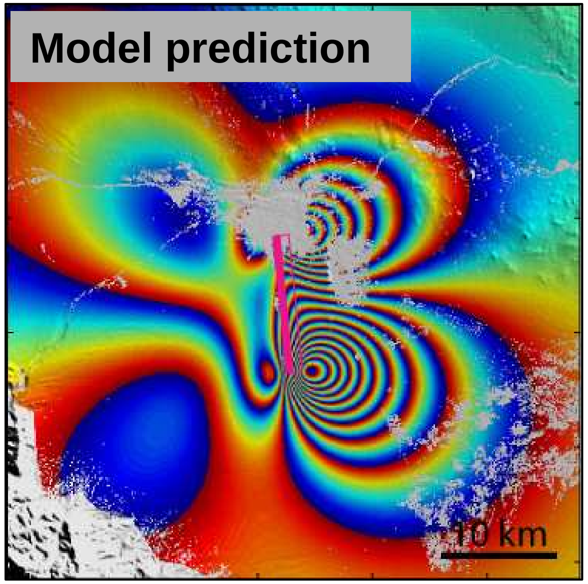

- Fault length: 12 km
- Fault depth: 1.3 km
- Strike: 5 degrees W of N
- Dip: 81 degrees to the east!
- Strike-slip ~ 2 m
- No dip-slip

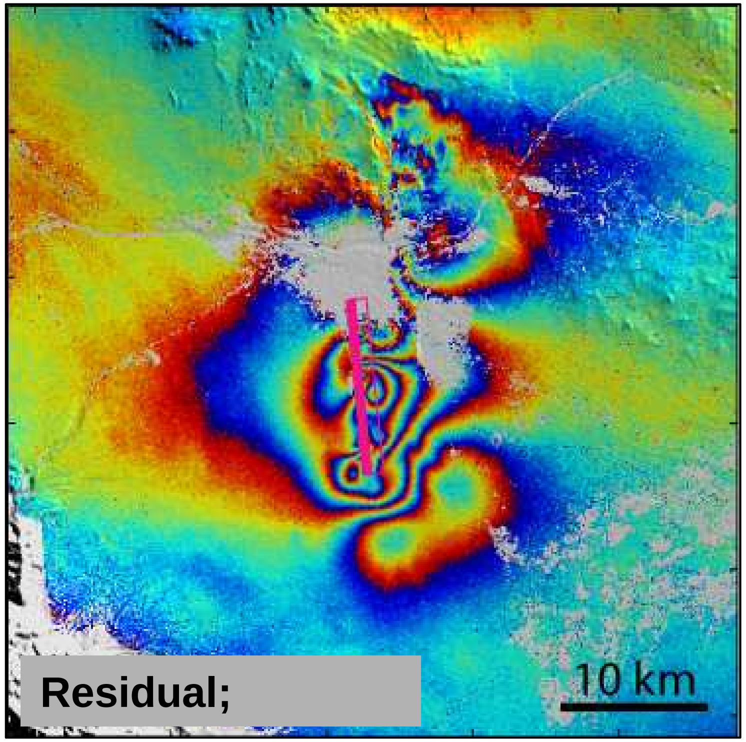

Geometry from aftershock data

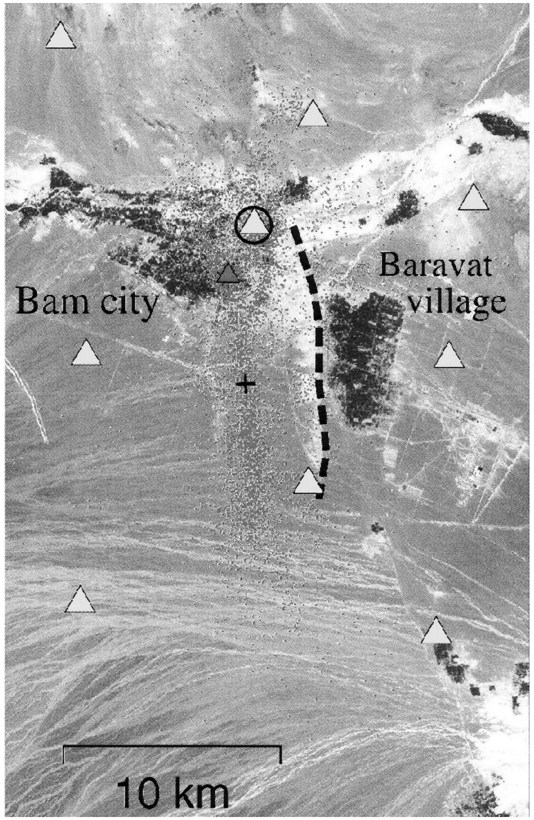

From Nakamura et al., 2005

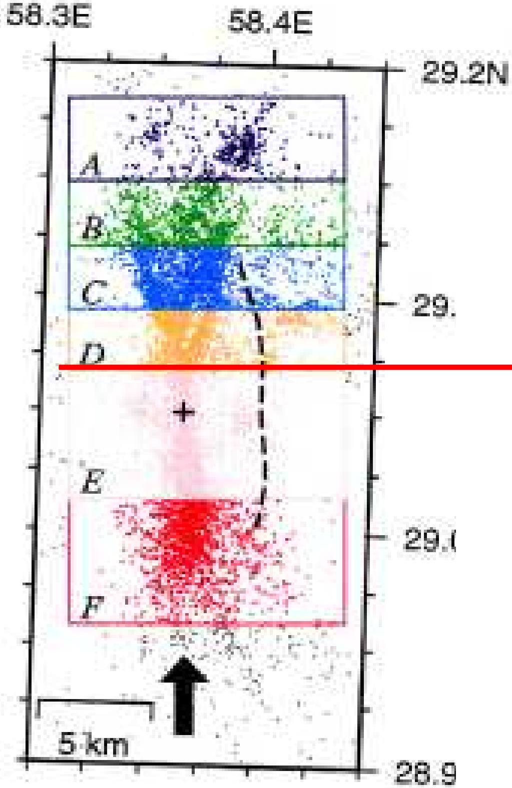

- **Aftershock locations show strike slightly west of North**
- **Near vertical fault, perhaps with small dip to the west**
- **InSAR-inferred fault-dip inconsistent with aftershocks**

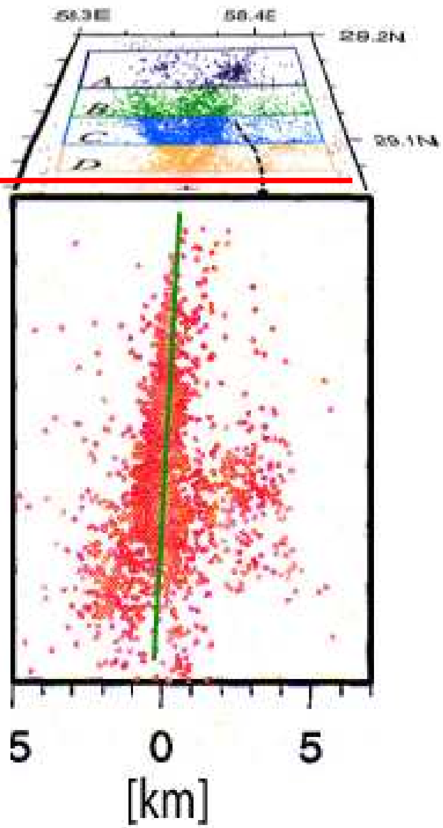

Fault Slip Distribution

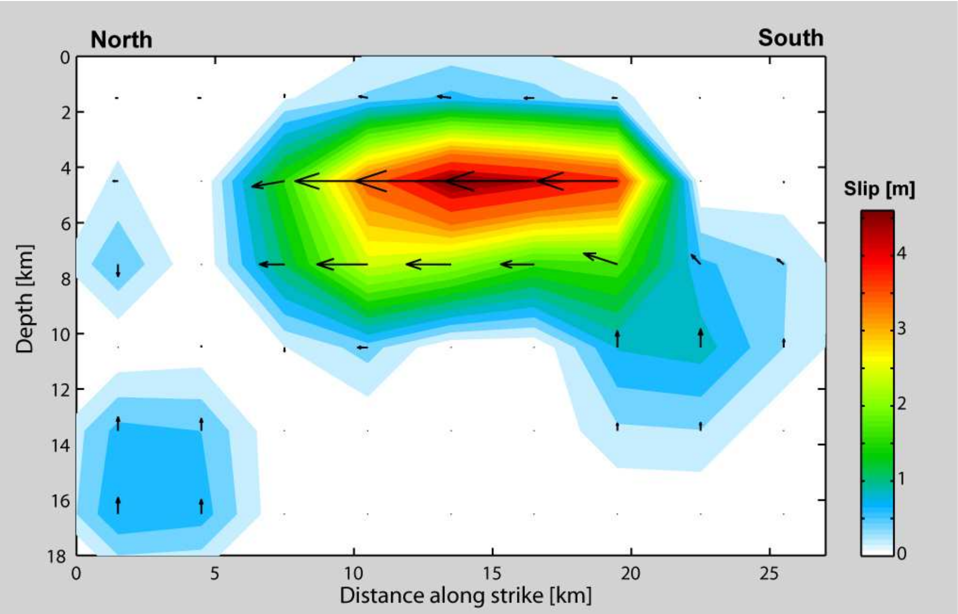

- Fault geometry determined from aftershocks
- Solve for variable slip on fault plane (linear inversion for fixed geometry)
- Maximum strike-slip ~ 4 m
- Max. dip-slip (west side up) ~ 0.4 m

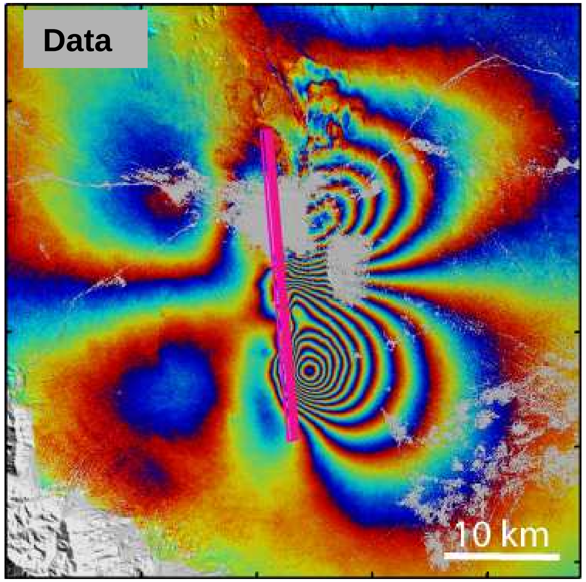

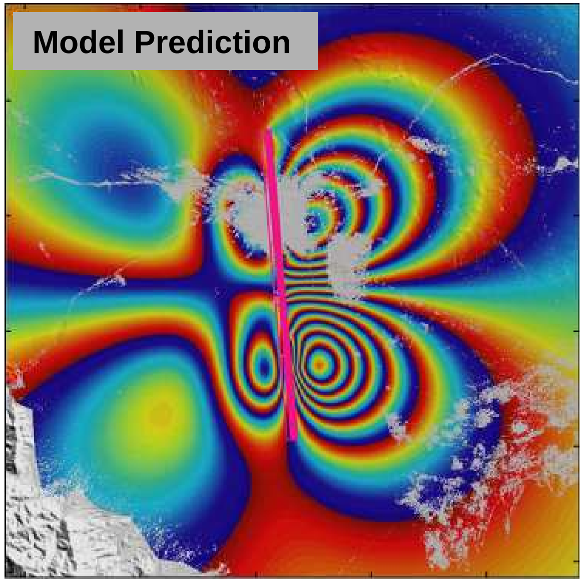

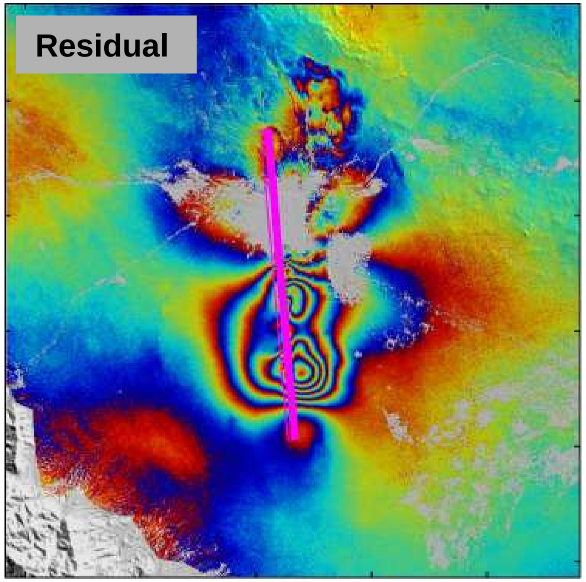

Inversion of Teleseismic Data

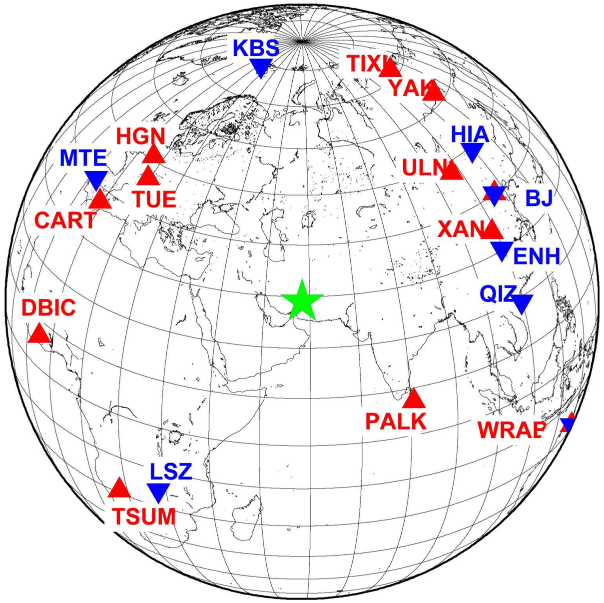

- Strike: 175
- Rake: 150
- Dip: 84

- P-waves at 11 stations, SH-waves at 8 sites
- P-waves @ 1Hz filtered, SH-waves @ 0.4 Hz
- "Uniform" azimuthal coverage and data quality
- Step 1: Point-source modeling
- Step 2: Non-linear, finite-source inversion, solving for slip, rake, rupture time in multiple time windows

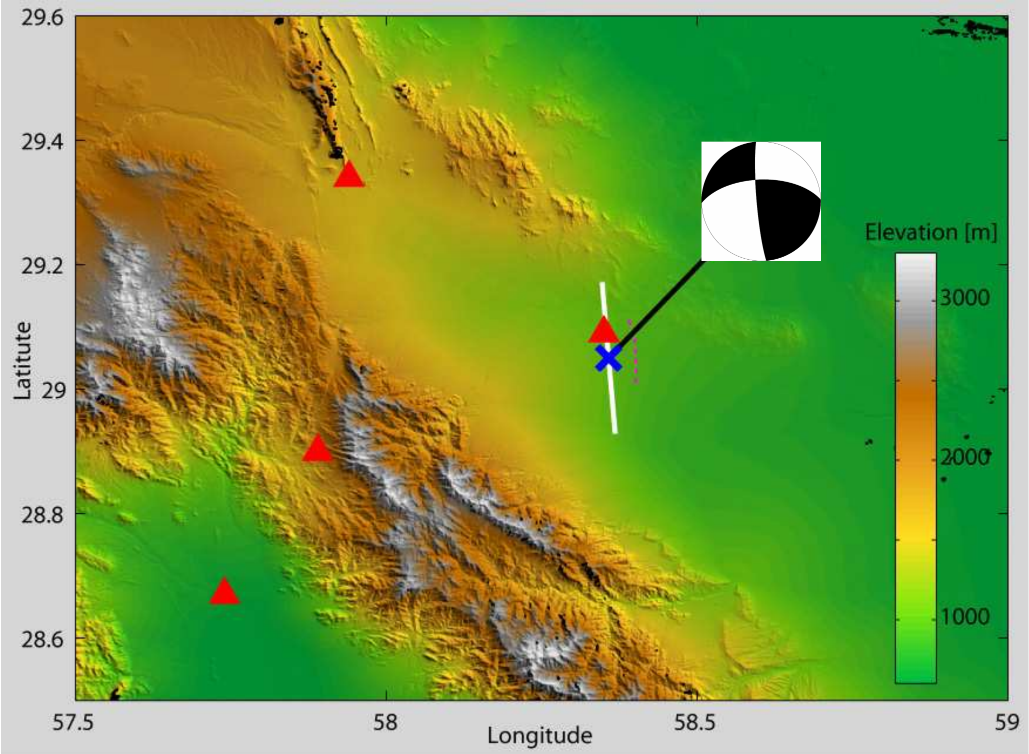

Inversion of Teleseismic Data

- 5 solutions that fit the teleseismic data almost equally well
- Slip at hypocenter well constrained (Δσ ~ 30 MPa), other regions with large uncertainty
- Rupture times indicate fast propagation in an up-dip direction towards city of Bam

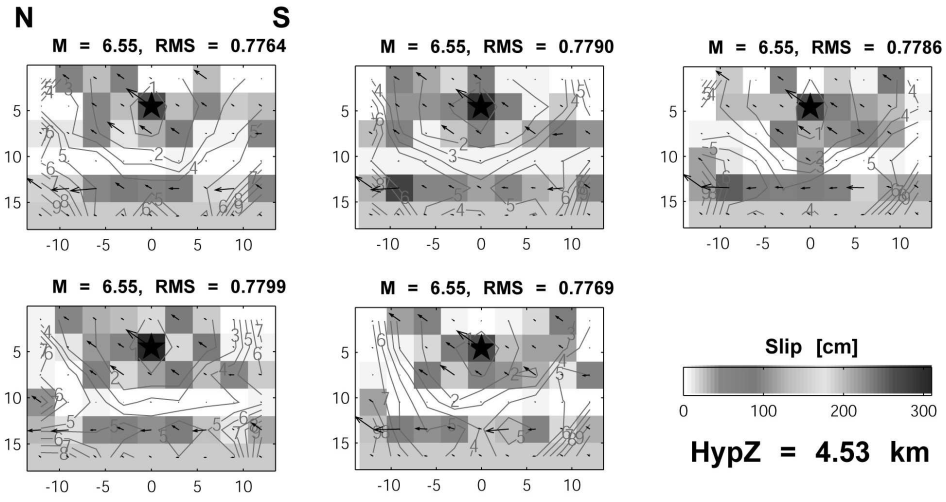

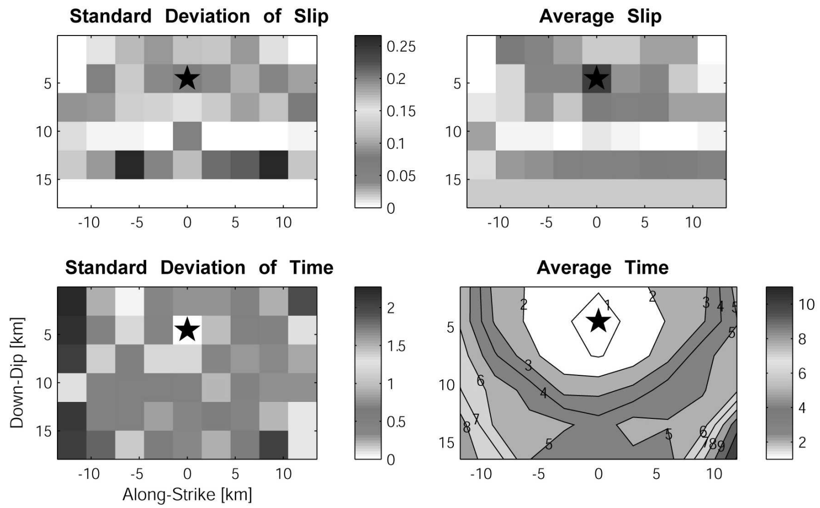

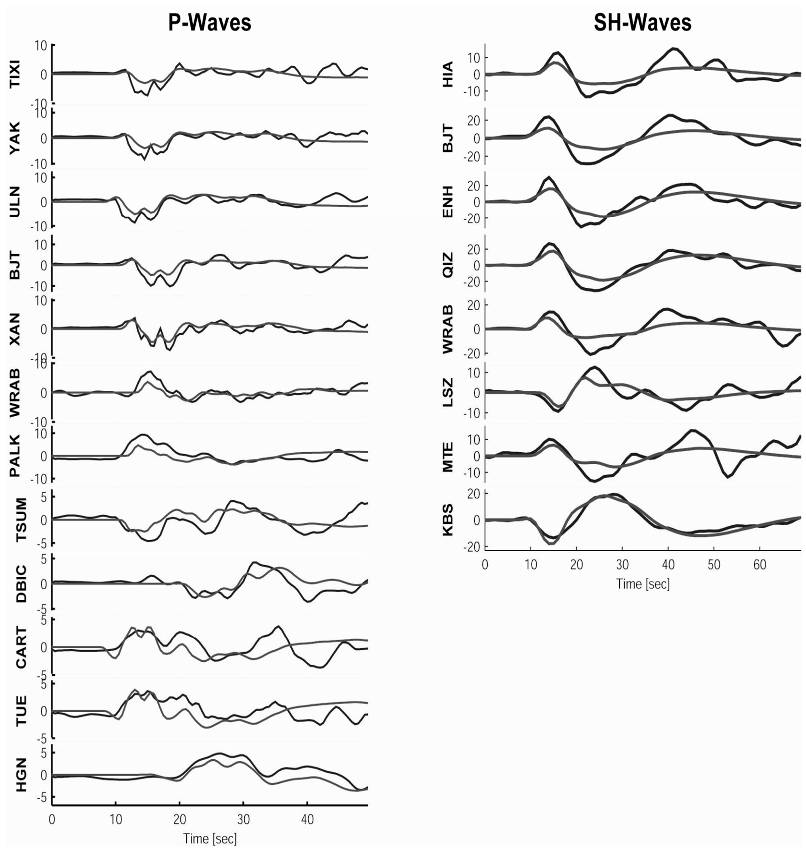

"Joint" Inversion of different data sets

At this point, … studies perform a j… ….

- How to defin…
- How to choo…
  - e.g. minimiz… will image source variabilit… …w them all into one big …
- Should we a…

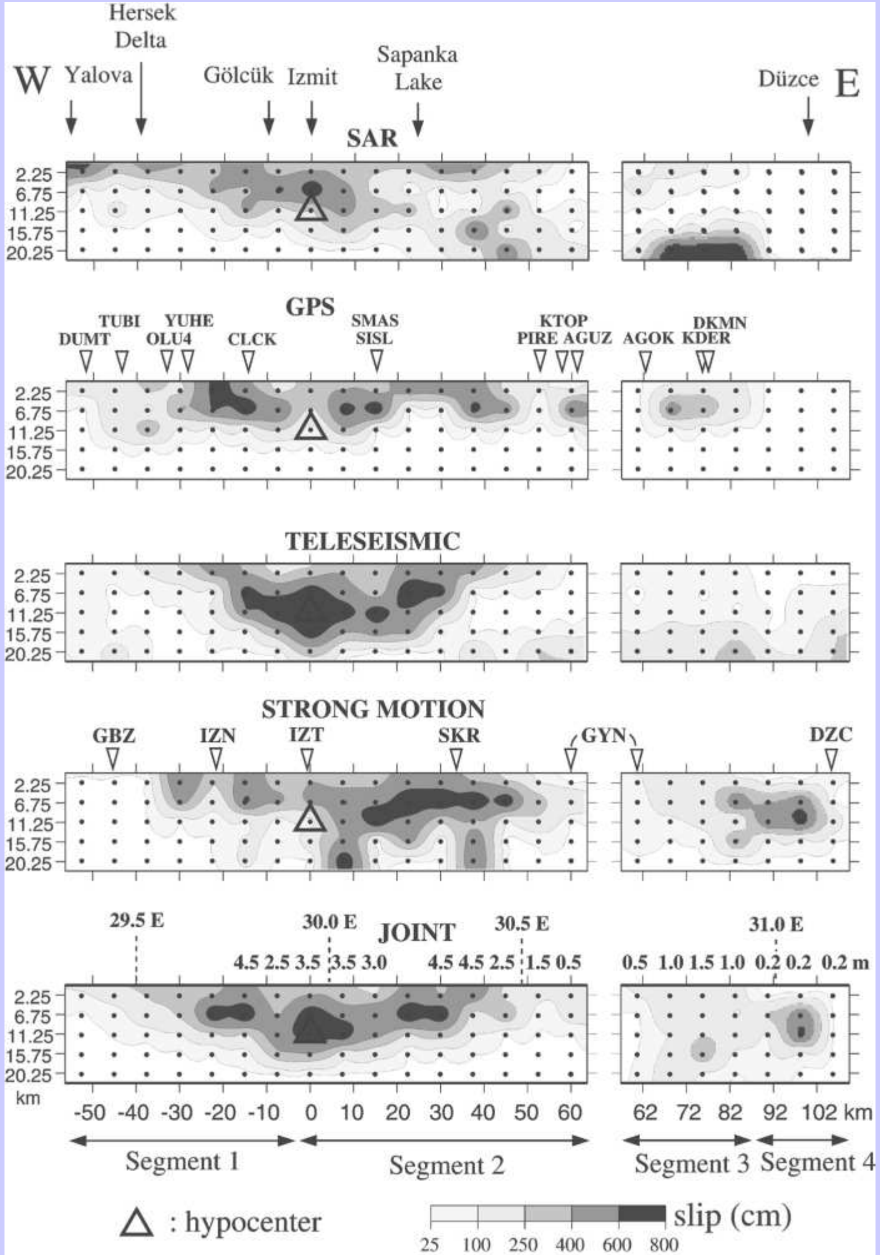

Delouis et al , 2002

We choose a … …t data sets:

- How well ca…
- Does the tel… …easurements?
- Can we mod… …ion)?

“Cross-Validation” I

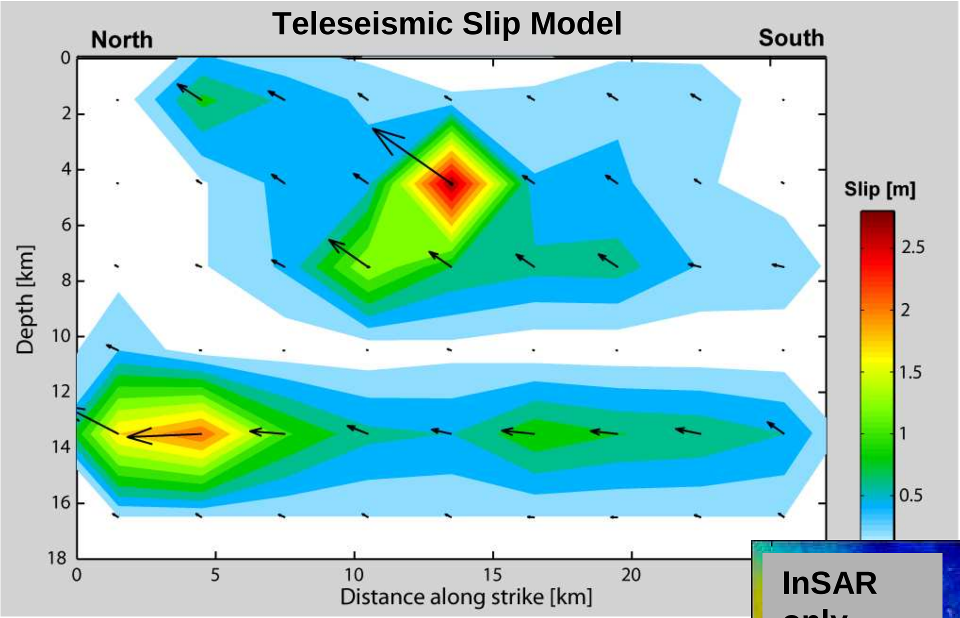

- How well does the teleseismic slip model reproduce the InSAR data ?

→ Large residual, ie. the teleseismic slip model does not fit the InSAR data !

→ Misfit decreases if the dip-slip contribution of the model is neglected

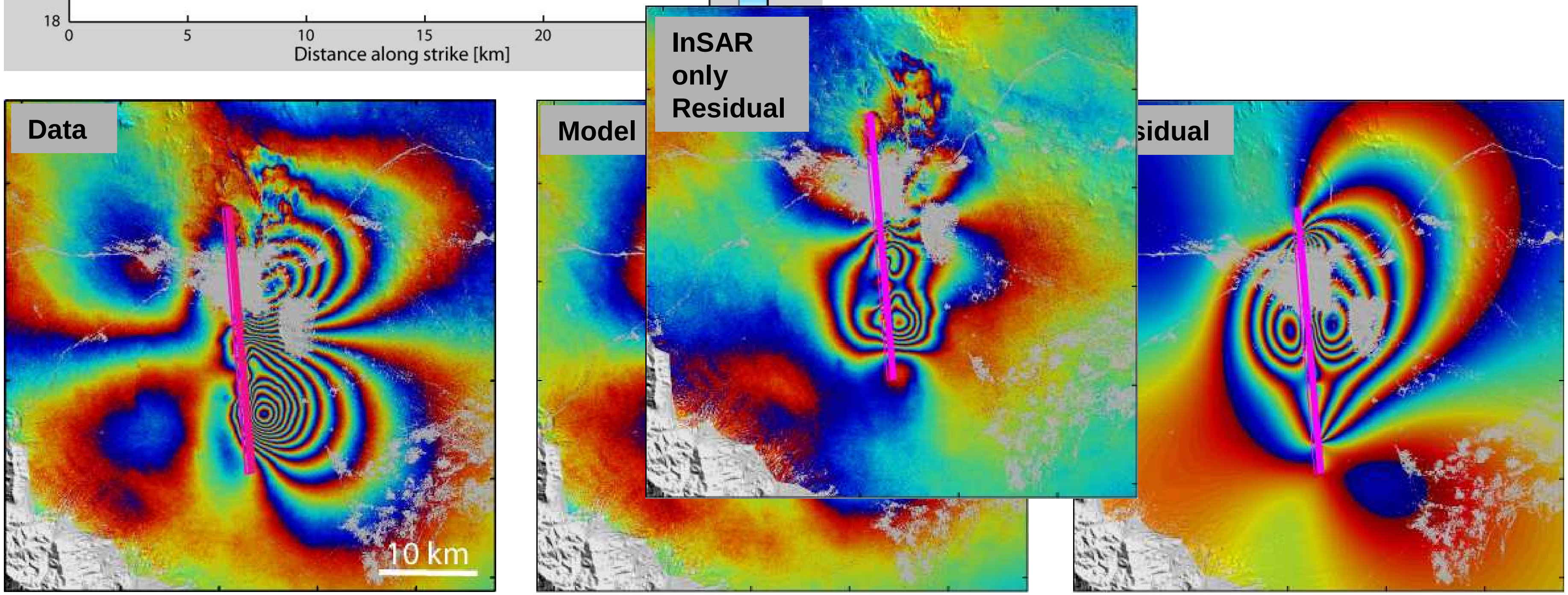

Eidgenössische Technische Hochschule Zürich

"Cross-Validation" II

Using the InSAR slip map to constrain the teleseismic inversion (allowing ±25-50% deviation), we solve for rake and rupture time. How well can we fit the teleseismic data?

"Constraint" InSAR slip model

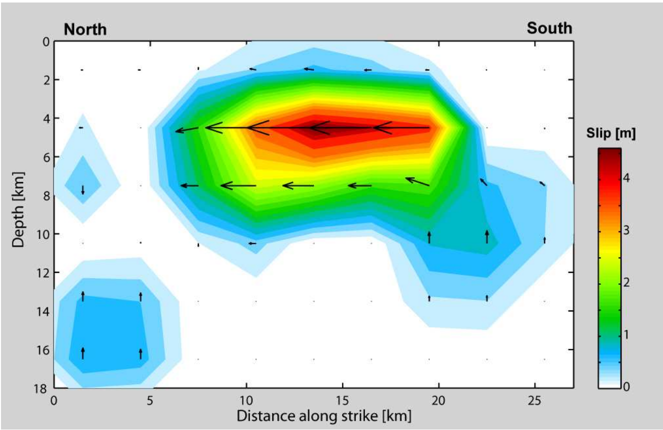

Resulting Teleseismic Slip Model

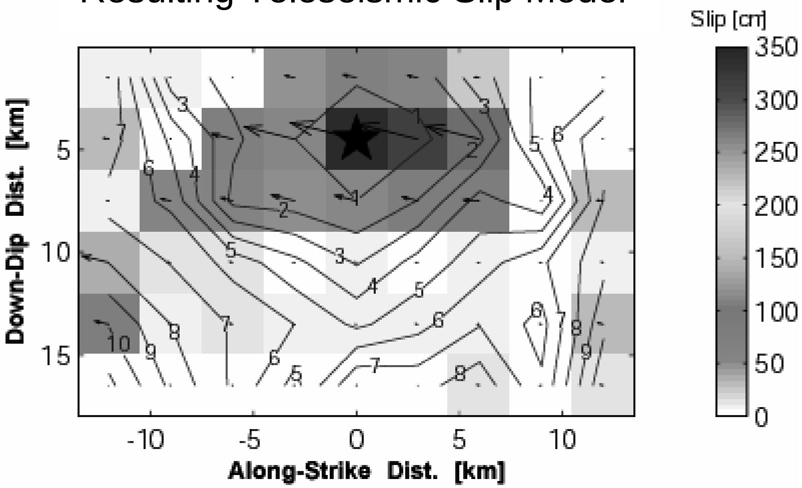

→ Solution "wants" some dip-slip
→ rupture times indicate lower rupture velocity
→ RMS misfit increases by ~ 10%
→ Some stations poorly reproduced

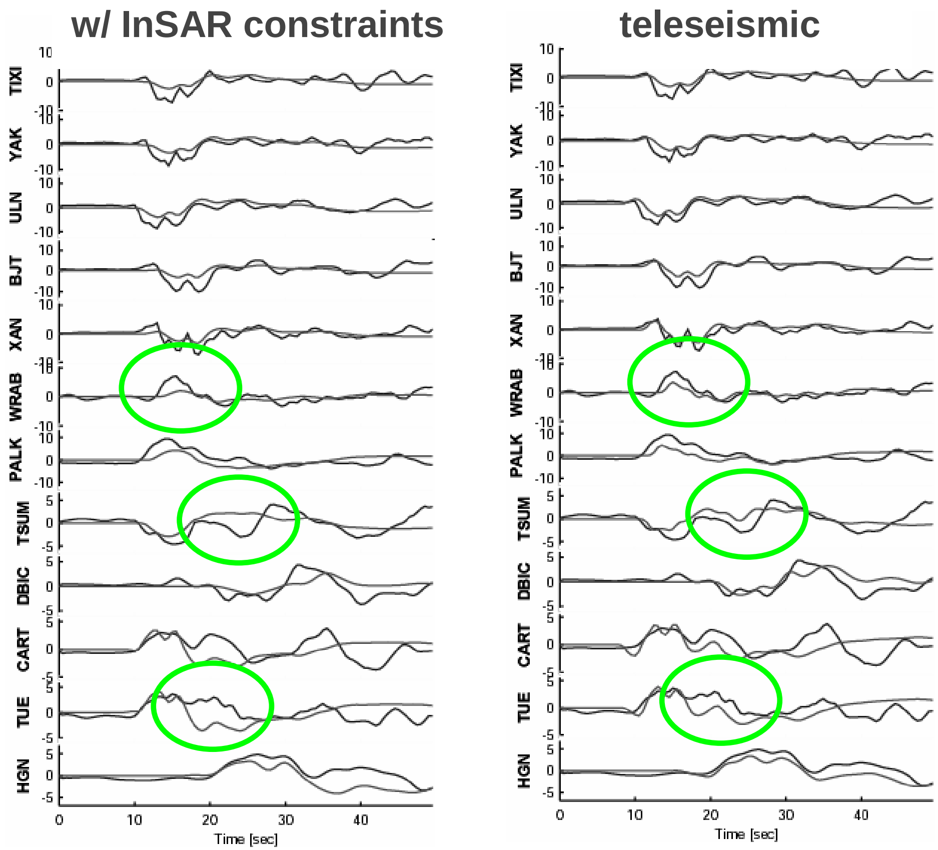

"Cross-Validation" III

Using the teleseismic source model, how well can we "predict" the near-source motion?

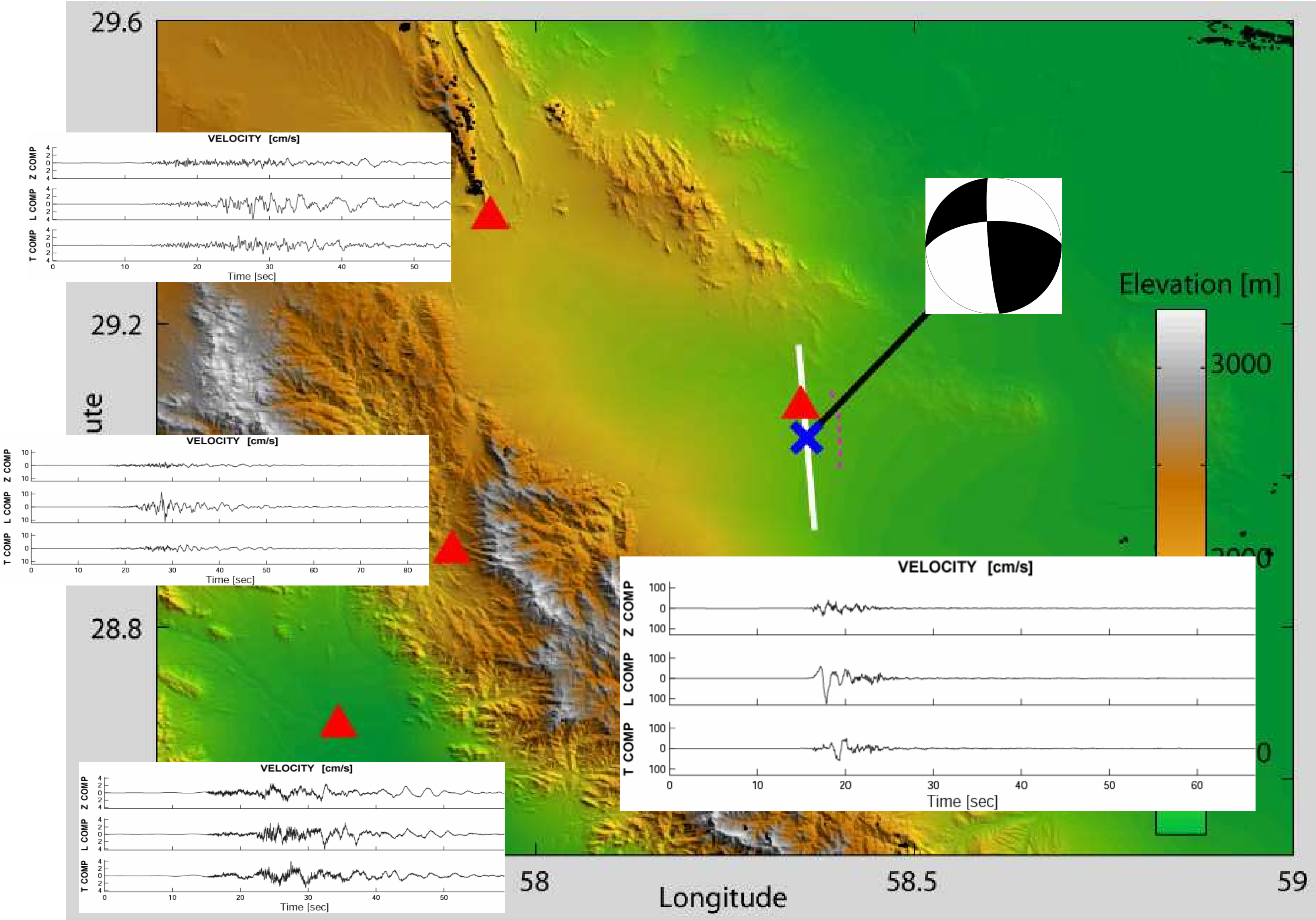

Strong Motion Data courtesy of BHRC, Teheran

"Cross-Validation" III

Using the teleseismic source model, how well can we "predict" the near-source motion? Here we only look at the site in the city of Bam

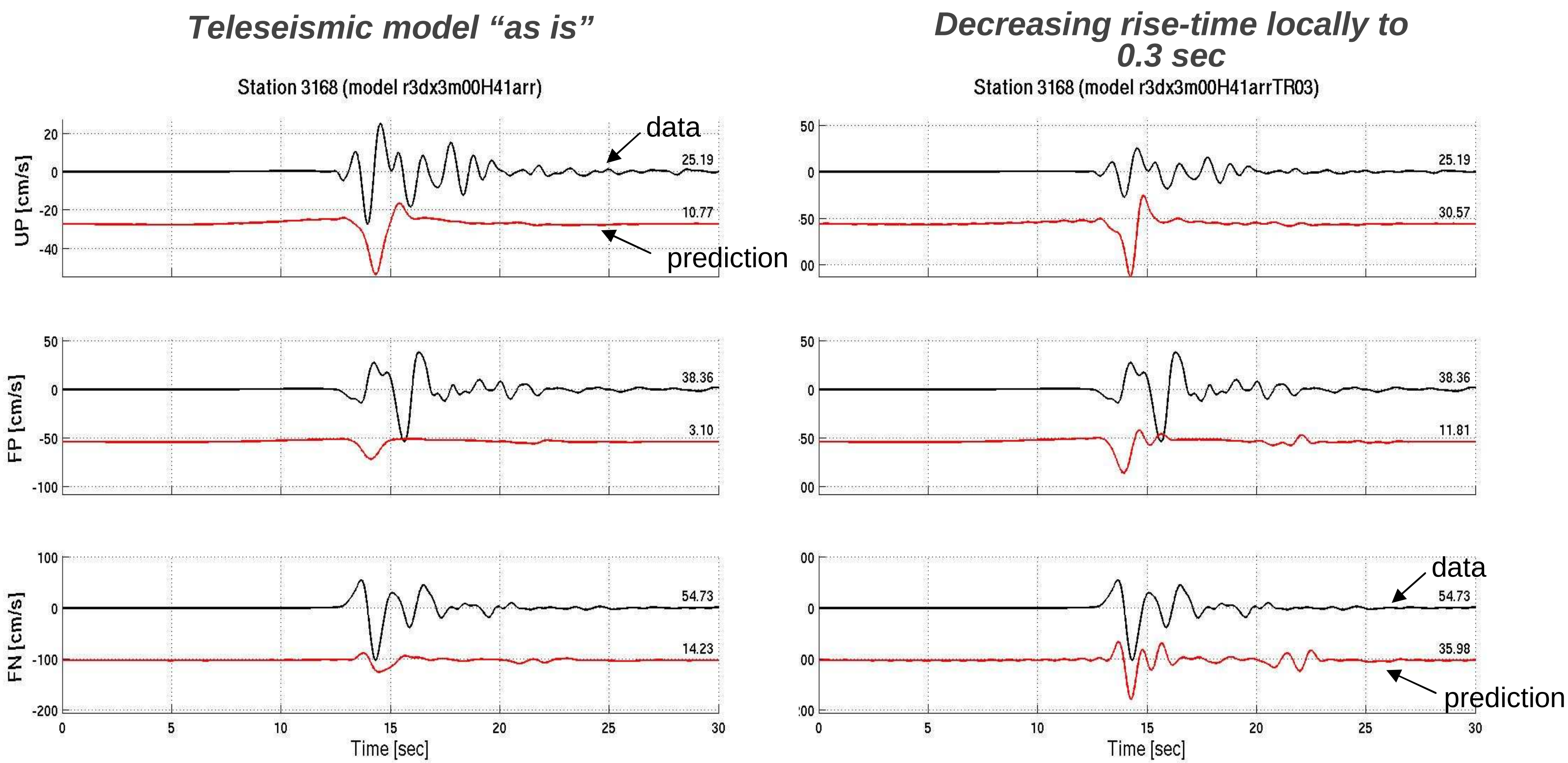

→ **Teleseismic slip model cannot reproduce near-source motion**

→ **Increasing the slip-velocity locally provides a better "match", but still not very satisfying**

→ **Since local-site effects are unlikely, we speculate that the "unusual" near-source motion in the city of Bam is due to some very localized source effect!**

Conclusions: BAM source modeling

► We find discrepancies between the InSAR slip model and the teleseismically inferred source-rupture model:

► The InSAR data cannot be adequately reproduced with the teleseismic slip solution; using the InSAR-slip as a constraint in the teleseismic inversion degrades the fit to teleseismic data significantly.

► Neither the InSAR- nor the teleseismic model explain the unusual near-source record in the city of Bam. Since there is no evidence for site effects, some localized source effect is the likely explanation.

► Source inversions using multiple data set should consider mutual validation tests; classical "joint" inversions suffer from the difficulties in determining the weights of the data sets

Validation of Source Inversion Methods

The preceding example, and our experience with the source-model database, shows that there is an urgent need to

► **test, compare and validate finite-source inversion methods that are currently in use or actively developed**

→ linear versus non-linear methods
→ misfit criteria used
→ data processing steps taken in the beginning
→ “code-internal” representation of the model (dependence of parameterization of grid, time-windows, slip functions etc)

► **report not only “one single best model”, or a small set of models for slightly different parameterizations, but try to estimate the actual uncertainty of the model parameters**

⇨ **SPICE blind-test for source inversion approaches:**
a multi-level “exercise” to test and validate source-inversion methods

SPICE Blind Test on Source Inversion

- Source geometry and station distribution chosen similar to the 2000 Tottori earthquake
- Synthetic seismograms are computed at 19 near-fault sites, assuming constant rupture velocity, constant rise time, simple slip-velocity function, but heterogeneous slip; these parameters are unknown to the source-inversion teams
- Wavefield calculated with discrete wave-number integration method (f_{max} ~ 3.0 Hz)
- Initially, the synthetics are noise-free; in the later stages, noise will be added and the above conditions on v_r, τ_r will be relaxed.
- Given: seismic moment: 1.43×10^{19} Nm
  strike, dip, rake: 150, 90, 180
  hypocentral depth = 12.5 km
  velocity-density structure

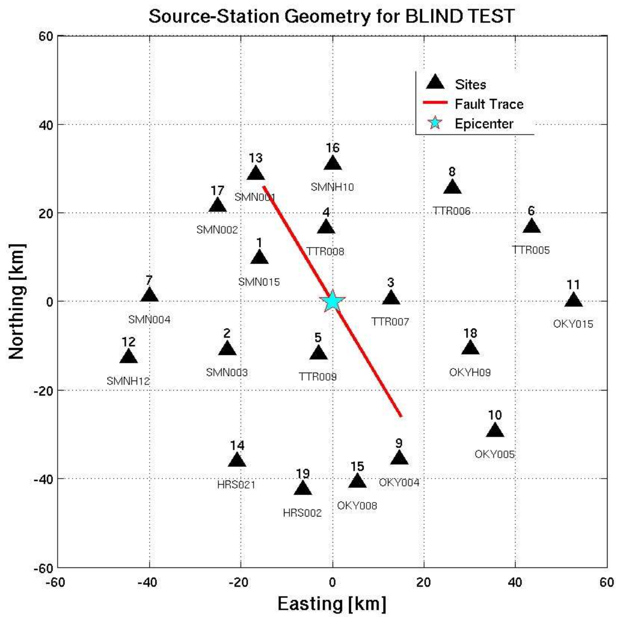

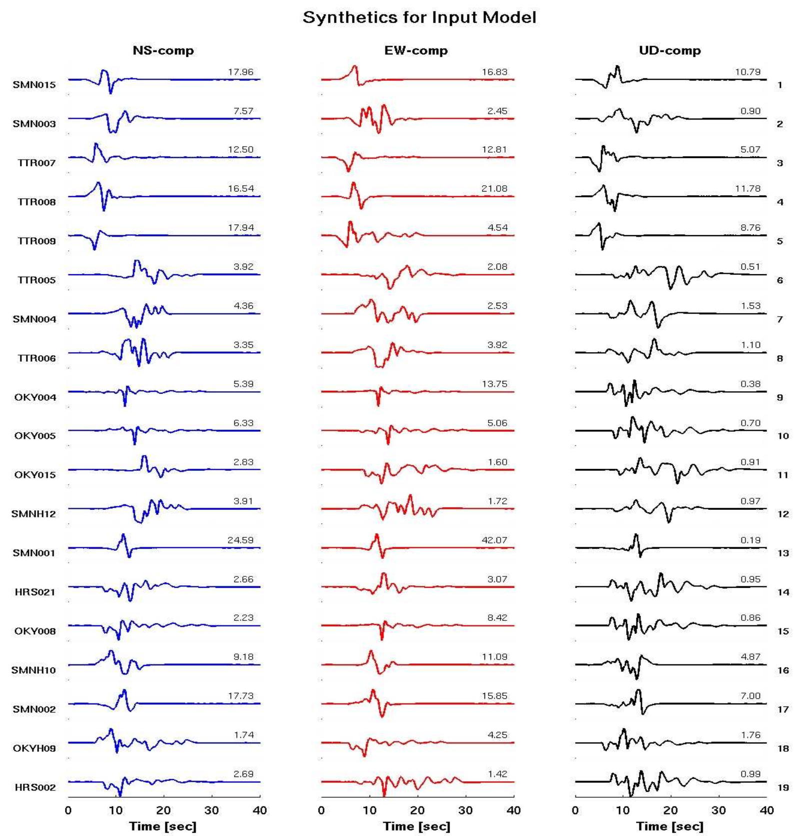

SPICE Blind Test on Source Inversion

So far, six source-inversion results were submitted, using different methods:

- **Model A: multiple point-source model (iterative moment-tensor deconvolution), GF's with Axitra (f_{max} = 1 Hz), [1 x 1] km large subfaults, solving for final slip by some search algorithm**

- **Model B: Non linear inversion using a neighborhood algorithm (Sambridge, 1999); GF's with Axitra (f_{max} = 1 Hz); [2.5 x 2.7] km large subfaults, solving for final slip and rupture velocity, minimizing L_2-norm**

- **Model C : Isochrone back-projection of high-frequency displacements (up to 1Hz); [1 x 1] km subfaults, solving for slip and rupture time, minimizing L_2-norm for <u>6 stations</u> only**

- **Model D: Non linear inversion by simulated annealing, L_2-norm fitness function with minimization of the total seismic moment, no smoothing; GF's with Bouchon code, [5 x 5] km large subfaults, solving for final slip using <u>only 6 stations</u>**

- **Model E: linearized inversion for slip using Gaussian basis functions, L_2-norm minimization (with positivity constraint), [1 x 1] km subfaults, solving for final slip**

- **Model F: Non-linear inversion with evolutionary algorithm, using a frequency-domain fitness function, GF's with CompSyn, [3 x 3] km subfaults, solving for slip and rupture time.**

Blind Test on Source Inversion

► Inversion Results 1: Estimated rupture velocity and rise time; overall slip-value distribution

- **Estimates of rupture velocity in the expected range; one solutions falls off by significantly under-estimating v_r**
- **Estimates for rise time τ_r also in the expected range, though generally biased high by ~20 %, perhaps due to waveform filtering at ~1Hz**
- **The resulting slip-value distributions are generally quite different amongst each other, and also with respect to the input distribution..**

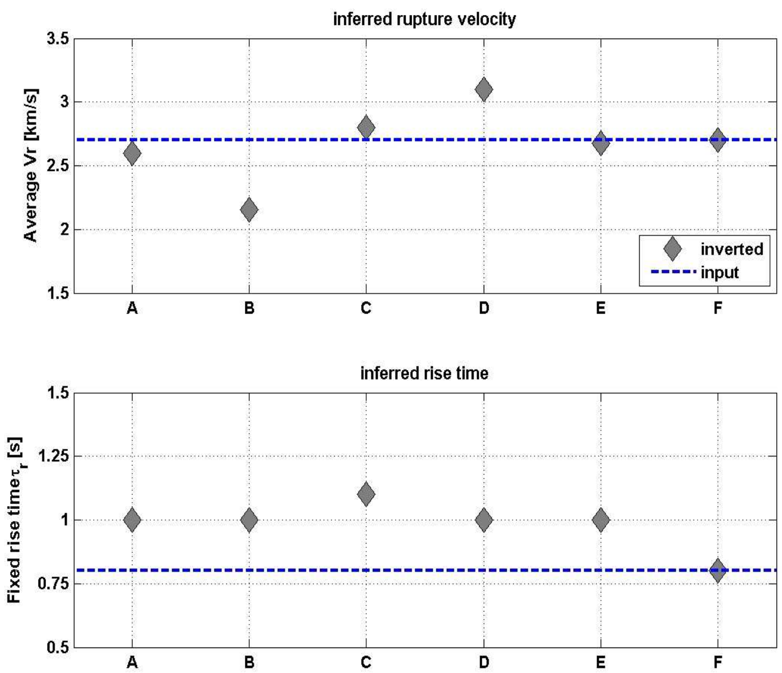

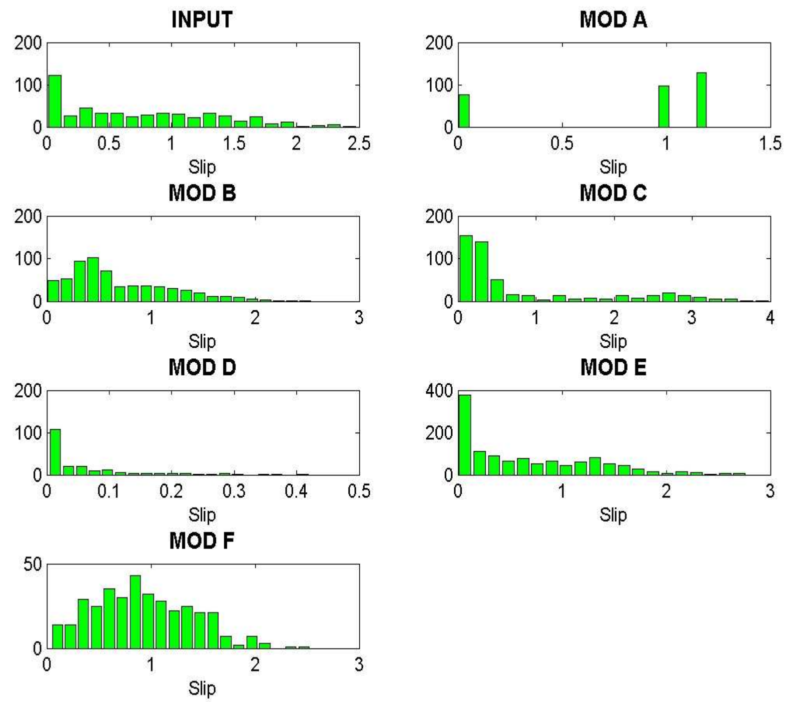

Blind Test on Source Inversion

► Inversion Results 2: Slip on the fault plane

- Resulting slip distributions are very different from each other, but also w.r.t. the input model
- Only two (perhaps three) solution(s) “match” the input model by visual inspection
- The comparison between the synthetic waveforms and those of the inverted models seems to indicate a “very good fit to the data” in all cases (i.e. by visual inspection)

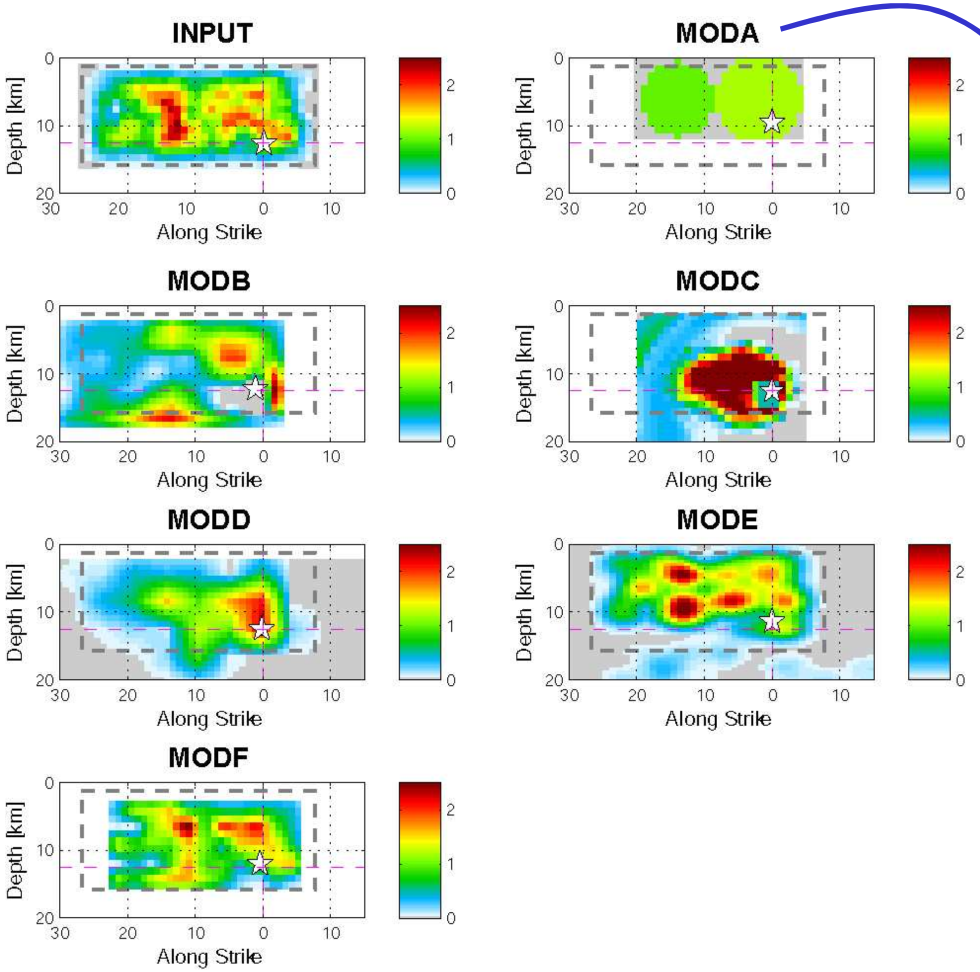

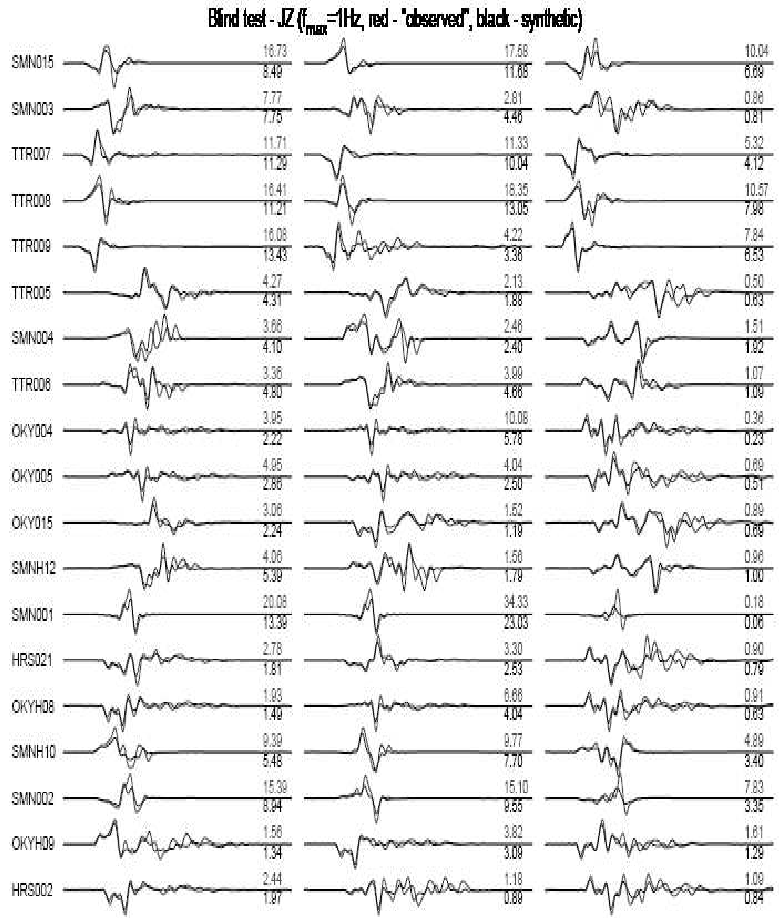

Blind Test on Source Inversion

► Quantitative comparison of slip models, I

- We examine the 2D-cross-correlation function between the input and the inverted models
- To calibrate the results, we first test a purely random field and a random, but correlated field
- Three out of six inversion results are NOT much better than a random, but correlated model!
- For three cases we obtain a correlation coefficient of ~ 0.9, while the lag is small (~ 2 km)

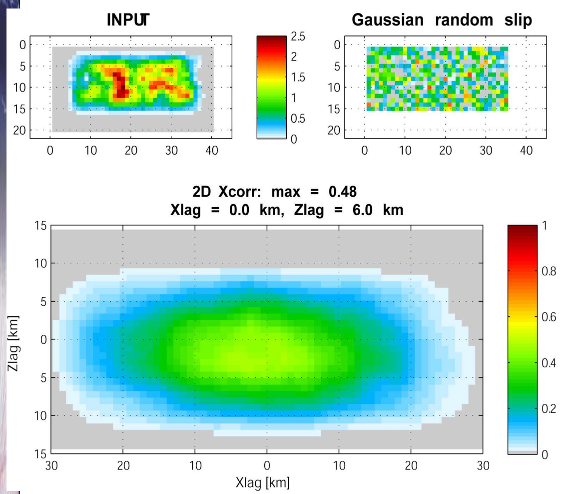

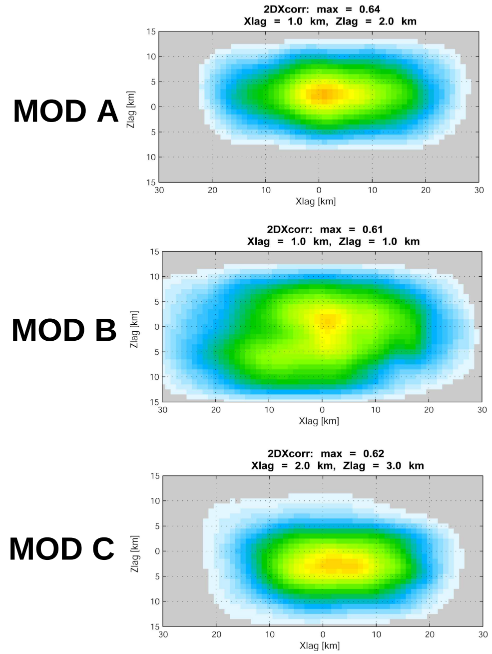

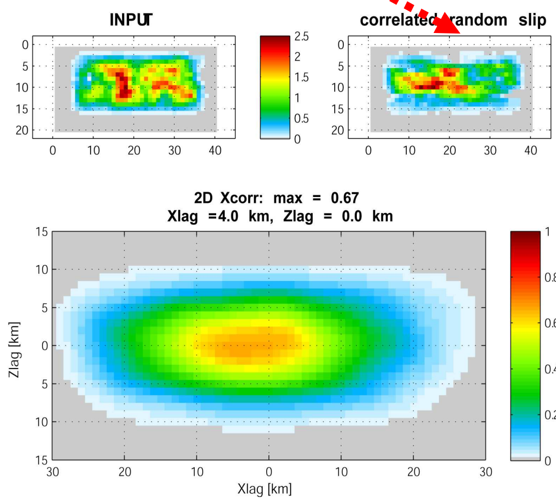

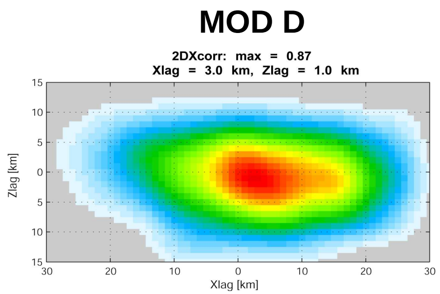

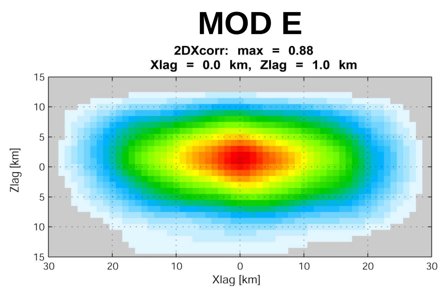

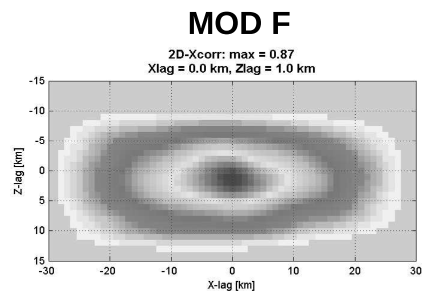

Blind Test on Source Inversion

► Quantitative comparison of slip models, II

- **Additionally, we examine the spectral characteristics of the input and inverted models to asses the scale-lengths up to which they agree with each other**

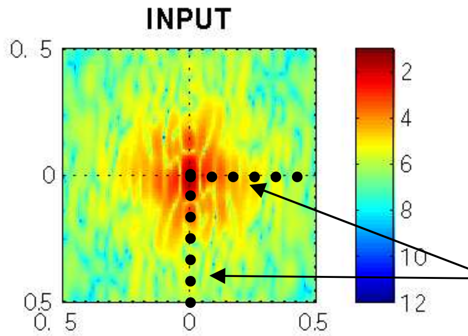

Two-dimensional wave number spectra of slip models, computed on square lattices (128 × 128 points);

next we analyze the 1D-spectra in each direction at $k_{x,z}$ = 0.

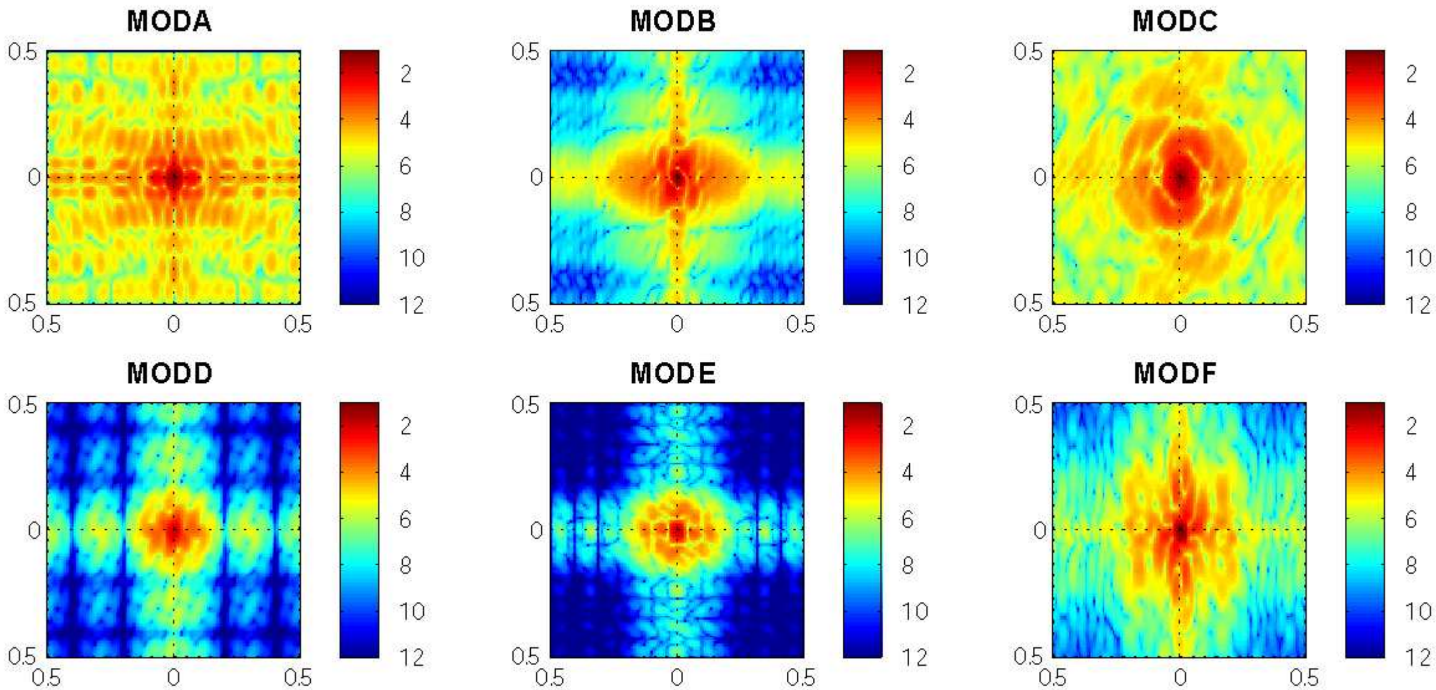

Blind Test on Source Inversion

► Quantitative comparison of slip models, II

- Additionally, we examine the spectral characteristics of the input and inverted models to asses the scale-lengths up to which they agree with each other

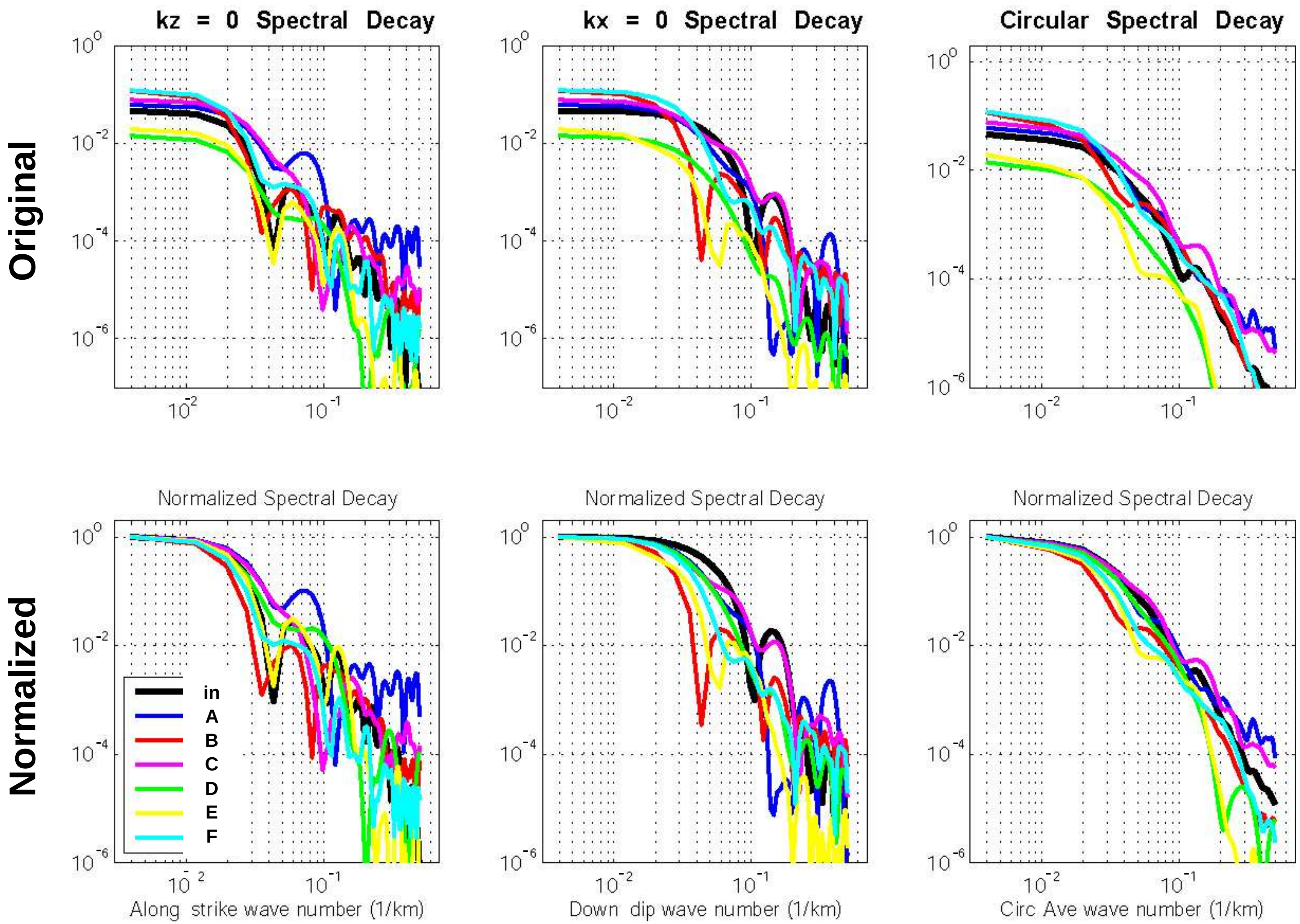

Spectral decay roughly consistent for wave-length ~ 5-10 km;

At smaller scales, the models deviate significantly, in that some have faster decay (smoother slip), others slower decay (rougher slip) than the input model (black line)

Blind Test on Source Inversion

► **The first solutions for the blind test were surprising**

- **Despite the apparent simplicity of the input model (and hence the seismograms), the inversions could not resolve the slip very well; uncertainties in rupture velocity and rise time on the order of 10 and 20 %, respectively**
- **Despite the differences among all inversion solutions, the predicted waveforms are remarkably similar, and result in rather low misfit values (generally L_2-norm)**
- **Three out of six inversion results are, statistically speaking, NOT better than a random model with somehow correlated slip!**

► **This exercise has basically just started (i.e. fall ’05), and will continue until the end of SPICE (and likely beyond). We will make the problem increasingly harder by**

→ **allowing for variable rupture velocity, rise time, rake angles**
→ **applying noise (or scattering operators) to the data**
→ **withhold information on geometry, moment-tensor solution, velocity-density model**

► **Incorporate non-SPICE researchers; interested groups (so far Grenoble, UC Santa Barbara, Berkeley) have started already, or signaled that they would …**

"The Future" in Source Inversion

► Current "state of art" (or "state of practice") in source inversion

- Kinematic source inversions for past earthquakes show that slip is heterogeneous at all scales, but these 'slip maps" may have large uncertainties
- Dynamic rupture modeling shows that rise time, rupture velocity are also highly variable. The increasing use of fully non-linear inversion approaches allows to image also the complicated temporal rupture evolution, but the uncertainties are again large.
- Green's functions are usually calculated for semi-known velocity structures (mostly 1D) up to frequencies of ~1 Hz; for higher frequencies, some approaches use empirical GF's
- Are any of the kinematic models any good, considering all the complexity from rupture dynamics, incompletely known velocity-density structure in the source region, and less-than-optimal data distribution?

► Innovative approaches to earthquake source imaging

- Rigorously investigate and quantify the model-parameter uncertainties
- Consider alternative, physically consistent slip-velocity functions
- Consider constraints from rupture dynamics
- What is the "optimal" experimental set-up to reliably image earthquake source parameters

→ **Multi-scale inversion (by re-normalization)** (Ide and Aochi, 2005; Uechida and Ide, 2006)
→ **Dynamically constrained source inversions**
→ **Inversion for dynamic source parameters using the crack-tip equation of motion.**

ETH Eidgenössische Technische Hochschule Zürich

Multi-Scale Inversion

► **An earthquake starts on a small nucleation patch from which the rupture grows – over several stages (or space-time scales) – to its final size**

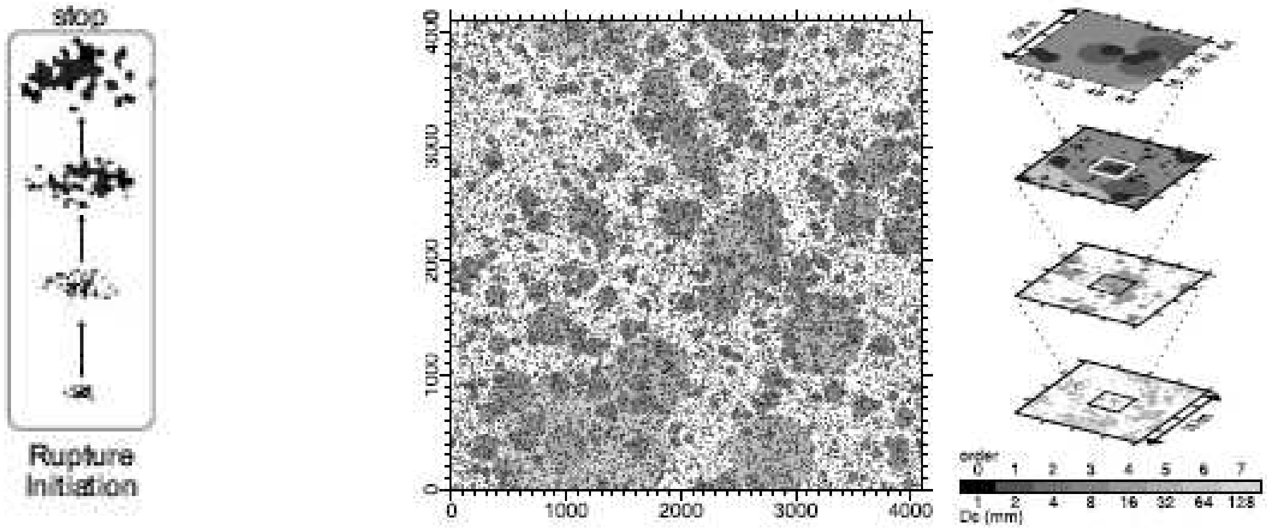

Ide and Aochi, 2005

- **Aochi and Ide (2004) and Ide and Aochi (2005) have developed a re-normalization scheme to model dynamic rupture propagation on a planar fault surface, considering fractal distributions for fracture energy . Only a limited number of events grew out of the nucleation patch, many stop “prematurely” to form a small (M~3) or moderate (M~5) events, while a small number of events grew into a large earthquake (M~6.5).**

- **Uchide and Ide (2006) have recently used that concept to map the 2004 mid-Niigata earthquake on different space-time scales, using EGF’s as Green’s functions for the small scale, and numerical Green’s functions for the larger scales.**

Multi-Scale Inversion

► An earthquake starts on a small nucleation patch from which the rupture grows – over several stages (or space-time scales) – to its final size

- Uchide and Ide (2006): At the small scales (~ 1sec, 4x4 km grid; 2.2 sec, 8x8 km grid), EGF's are used as Green's functions. At the largest scale (6 sec long expansion functions), numerical GF's are computed for an assumed velocity model.

- The governing linearized equations are combined into one single, multi-scale observation equation, which is then solved with additional smoothing constraints, and the rupture process is estimated at all scales simultaneously.

- The inversion reveals a very complex initiation, with changing directivity at different times. The final slip distribution is similar to previous "mono-scale" inversions for the earthquake, but shows more small-scale variability.

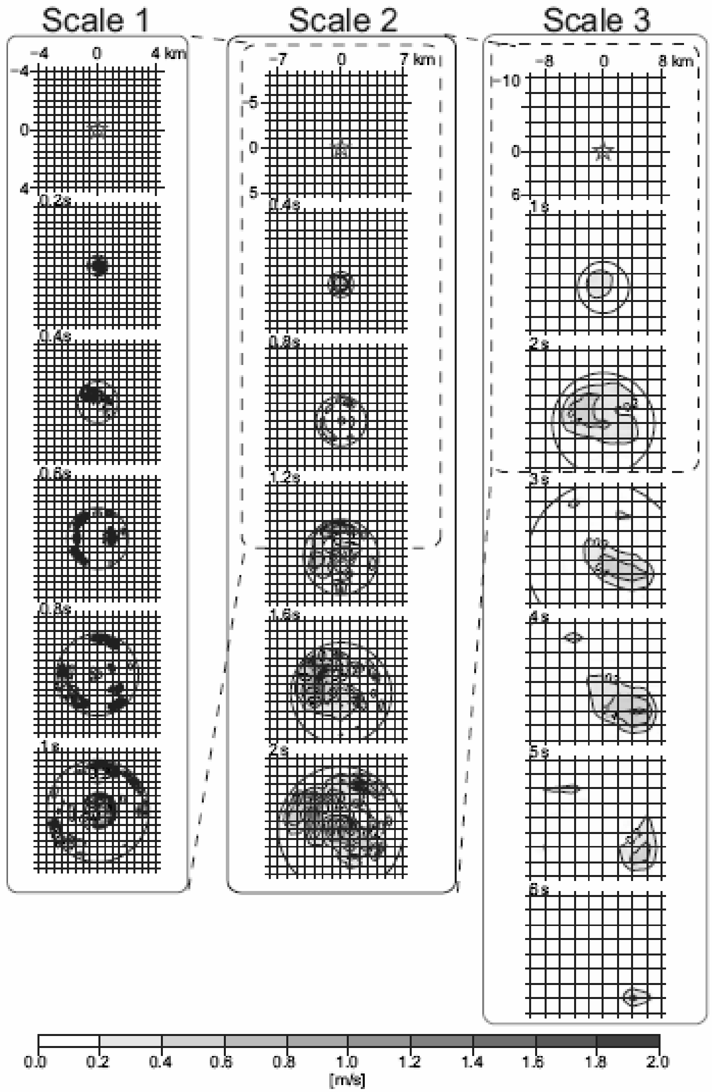

"The Future" in Source Inversion

► Current "state of art" (or "state of practice") in source inversion

- Kinematic source inversions for past earthquakes show that slip is heterogeneous at all scales, but these 'slip maps" may have large uncertainties
- Dynamic rupture modeling shows that rise time, rupture velocity are also highly variable. The increasing use of fully non-linear inversion approaches allows to image also the complicated temporal rupture evolution, but the uncertainties are again large.
- Green's functions are usually calculated for semi-known velocity structures (mostly 1D) up to frequencies of ~1 Hz; for higher frequencies, some approaches use empirical GF's
- Are any of the kinematic models any good, considering all the complexity from rupture dynamics, incompletely known velocity-density structure in the source region, and less-than-optimal data distribution?

► Innovative approaches to earthquake source imaging

- Rigorously investigate and quantify the model-parameter uncertainties
- Consider alternative, physically consistent slip-velocity functions
- Consider constraints from rupture dynamics
- What is the "optimal" experimental set-up to reliably image earthquake source parameters

→ **Multi-scale inversion (by re-normalization)** (Ide and Aochi, 2005; Uechida and Ide, 2006)
→ **Dynamically constrained source inversions**
→ **Inversion for dynamic source parameters using the crack-tip equation of motion.**

"The Future": Dynamic Source Inversion

► Dynamic source inversion

- ❑ Recently, Peyrat and OIsen (2004) have carried out a full dynamic inversion to map slip, slip-rate, and stress for the 2000 Tottori earthquake, assuming constant yield stress and uniform slip-weakening constitutive law. Their study estimates parameters at 24 points on the fault, using the full time histories of 12 near-source recordings (low-passed to 0.5 Hz), requiring more than 50'000 spontaneous dynamic rupture calculations …

- ❑ Why not work progressively in time, by using the isochrone-method?
  Starting from rupture nucleation, we track the propagating rupture front, searching for the optimum stress and fracture-energy configurations. The large-scale stress pattern can be constrained by inverting GPS/InSAR data. Initially we work on a small grid, and high spatial and temporal resolution; at later stages, this scheme will be "scaled up" (Ide and Aochi, 2005) to allow mapping the entire fault plane.

“The Future”: Dynamic Source Inversion

► Dynamic source inversion

<u>The isochrone method</u>: The S-wave arrival at a given station at any instant in time depends on the rupture propagation time and the travel times from points on the fault to the station.
The displacements in the seismograms, at each time, is then given by integrating along the isochrone.
With pre-computed travel times, we search for those distributions of stress-drop and fracture energy that would advance the rupture front to the appropriate position and provide the correct amount of slip.

The isochrone method has been used in the past for kinematic source inversions (e.g. Beroza & Spudich, 1988), but here we want to simply use the idea, and solve for dynamic parameters of interest.

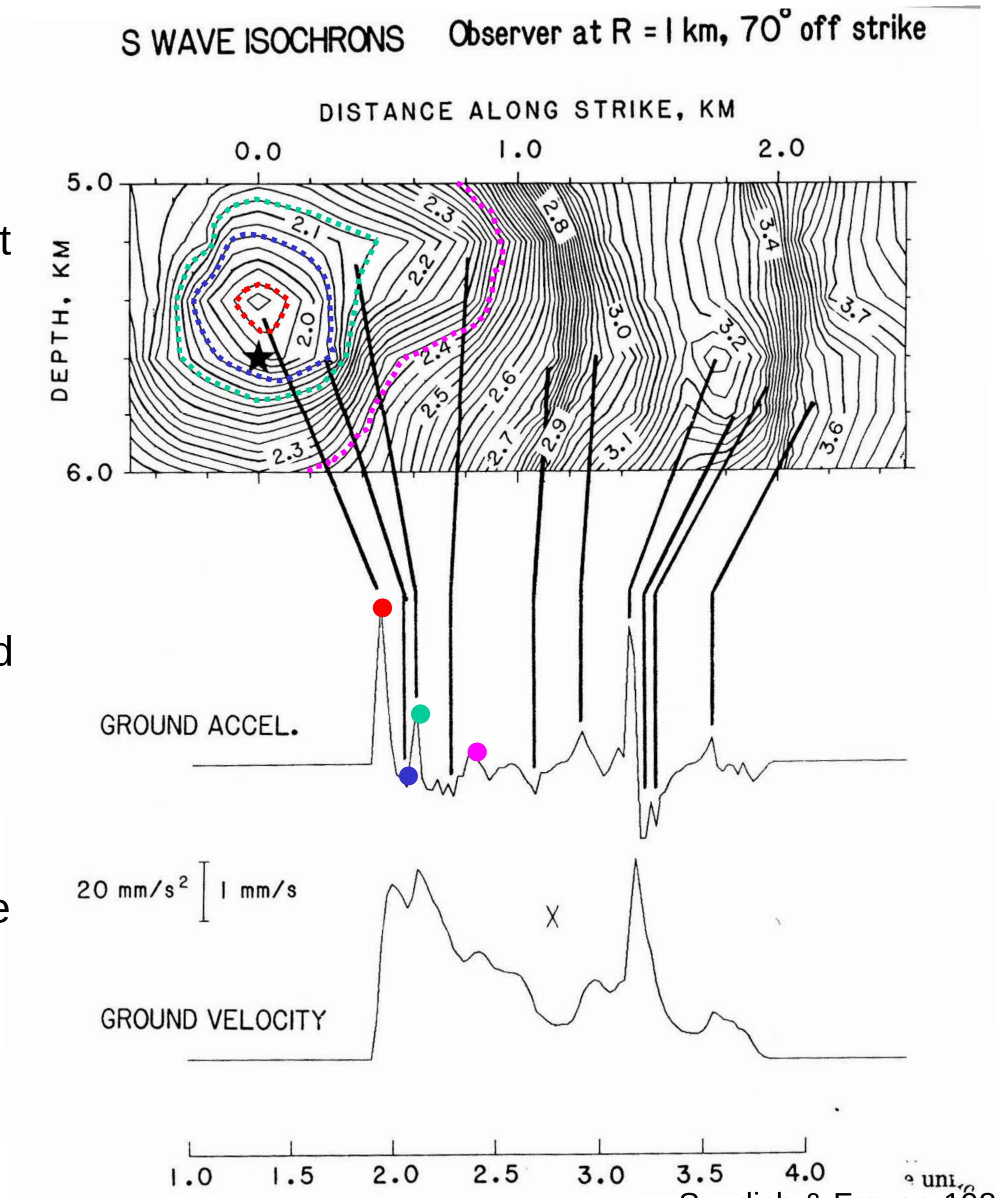

Spudich & Frazer, 1984

"The Future": Dynamic Source Inversion

► Dynamic source inversion

The crack-tip equation of motion:

• The growth of the rupture is ensured by the continued energy flux from unfractured material to the crack tip (for homogeneous material, once rupture has started, it will not stop). The energy flow G_{dyn} to the crack tip is dissipated in the process zone by "microscopic" inelastic processes: frictional weakening, plasticity, damage, etc.

• The crack-tip stresses are given by

$$\sigma_{ij} = K_n \frac{1}{\sqrt{2\pi r}} f_{ij}(\theta) + \sigma_{ij}^0 + O(\sqrt{r})$$

• The static stress intensity factor K_n depends on : rupture mode, crack geometry (size *a* and shape), remotely applied stress (tectonic load), stress drop $\Delta\sigma$.

• In many cases, the dynamic stress intensity factor can be written as

$$K_{dyn} = g(v_r) \cdot K_0(a, \Delta\sigma)$$

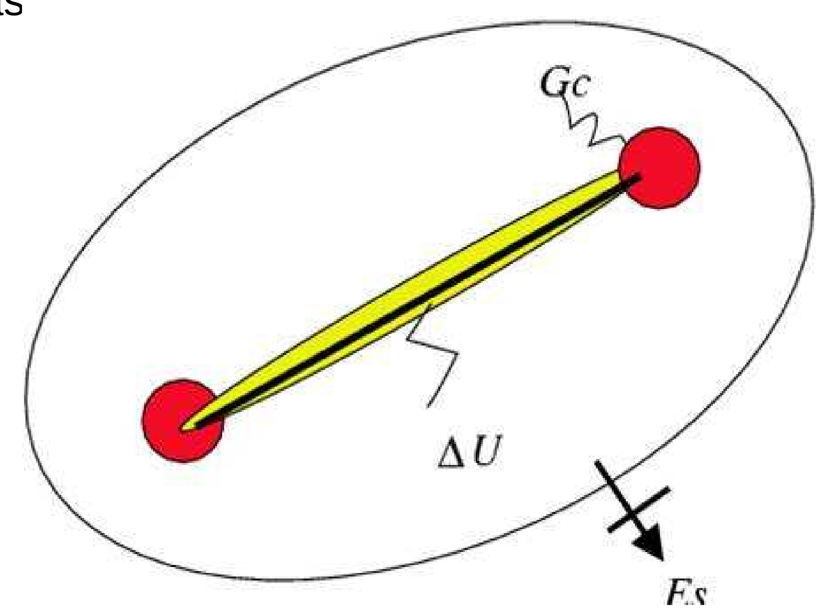

"The Future": Dynamic Source Inversion

► Dynamic source inversion

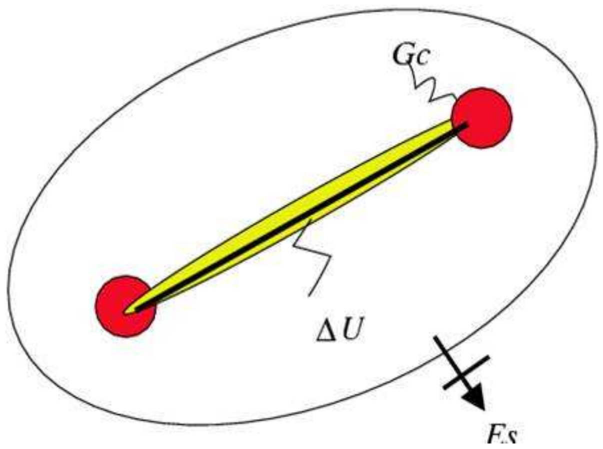

The crack-tip equation of motion:

• During rupture growth, potential and kinetic energy flows into the crack tip. This energy flux is related to K_{dyn} by (mode III)

$$G_{dyn}(v) = \frac{g(v)}{2\mu} K_{dyn}^2 \qquad g(v) = (1 - v^2/c_S^2)^{-1/2}$$

→ Combining with $K_{dyn} = g(v)\,K_0$, the dynamic energy flux can be factored as

$$G_c = G_{dyn} = (1 - v^2/c_S^2)^{1/2}\, G(a, \Delta\tau)$$

The dissipative processes at the crack tip may be lumped into a single mesoscopic parameter: the **fracture energy** $\mathbf{G_c}$ (energy per unit of crack advance)

Griffith criterion = energy balance at the crack tip

→ **crack tip equation of motion:**

→ **Given Δt and G_c , this equation can be solved for the rupture history (v_r and a)**

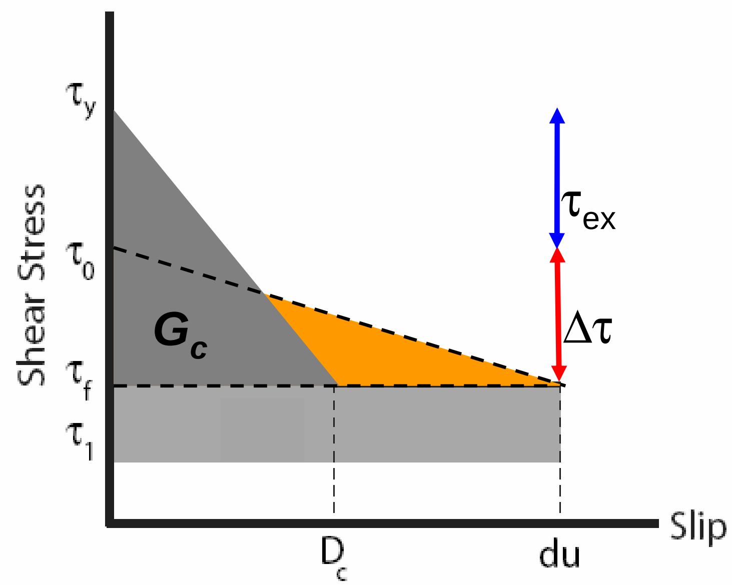

"The Future": Dynamic Source Inversion

► Dynamic source inversion

In practice: re-normaization

• Assume some "semi-random" stress drop on the fault plane whose larges-scale features could be constrained from InSAR/GPS inversion.

• Chose initial fracture energy distribution on the fault that promotes rupture nucleation and growth in a small region

• Perform dynamic rupture calculations on a small grid, search for the optimal stress – fracture energy configuration that fits the initial parts of the seismograms (use isochrone information)

• Once a (suite of) successful dynamic model(s) is found (within chosen misfit criteria), expand the computational domain to work on the later parts of the seismogram, i.e. rupture process.

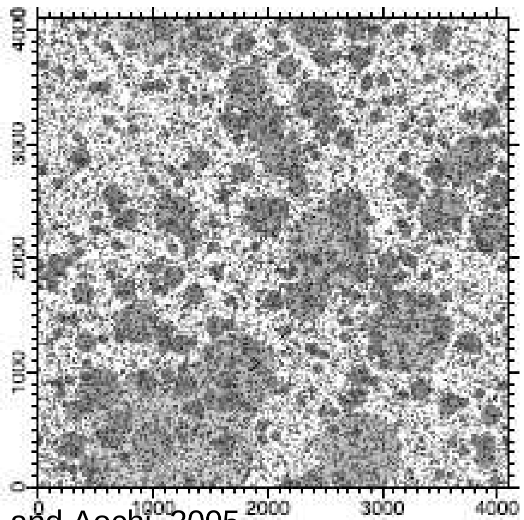

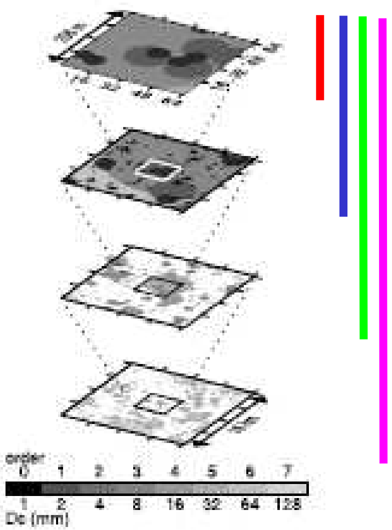

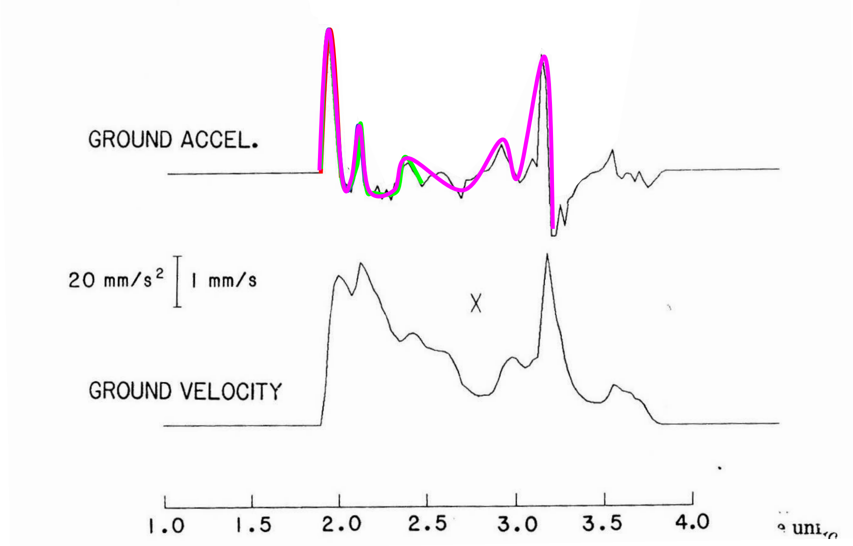

Ide and Aochi, 2005

SUMMARY

► Database of finite-source rupture models

This online database is extremely helpful for investigating the characteristics of earthquake source models, but also the variability of source-rupture models for a particular event from different research teams. Moreover, it can be used to develop other dynamic model for past earthquakes

► Source Inversion for the 2003 M = 6.6 Bam earthquake

Despite its moderate magnitude, this earthquake destroyed a huge building stock in the city of Bam, and claimed 26'000 lives. Studying the source process with three different data sets (InSAR, teleseismc, strong-motion) DID NOT provide a coherent slip solution – the cross-validation exercise pointed out that each model has considerable deficiencies. However, the unusual near-source record in the city of Bam seems to be related to a strong localized source effect

► Blind-test for source inversion approaches

Such tests are mandatory to truly assess the strength and weaknesses of the different approaches and to investigate the uncertainties in source-inversions.

► Towards dynamically constrained and dynamic source inversion

I think, with increasing computational power and a growing on understanding of dynamic rupture, we can move towards "smart" dynamic source inversions; still, kinematic source inversions will remain a powerful tool if we make the parameter search consistent with the basic principles of rupture dynamics.